Natural Resources Canada
Ressources naturelles Canada
Canada Centre for Remote Sensing
Centre canadien de télédétection
Canada
CSA ASC

Remote Sensing Based Vegetation Change Detection in Canadian Arctic and Subarctic National Parks

Results for Ivvavik National Park

ParkSPACE Project

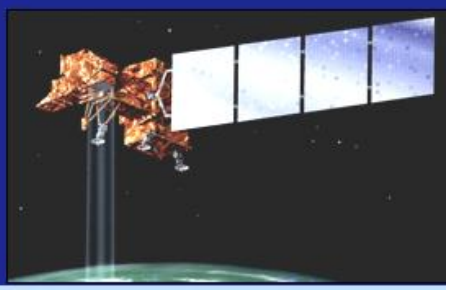

Remote Sensing Based Vegetation Change Detection in Canadian Arctic and Subarctic National Parks

Results for Ivvavik National Park

By Robert H. Fraser, Ian Olthof, Alice Deschamps, and Melanie Carriere

ParkSPACE Project

Prepared by Funding from the Government Related Initiatives (GRIP) Program of the Canadian Space Agency

Natural Resources Canada, Canada Centre for Remote Sensing
Parks Canada Agency, Ecological Integrity Branch
Ottawa, 2010

Purpose of Document

This document provides processing details and results for applying the methods described in a companion document “Protocol for Remote Sensing Based Vegetation Change Detection in Canadian Arctic and Subarctic National Parks” to Ivvavik National Park, one of four ParkSPACE pilot parks.

It provides details on satellite imagery and other input data used, park-specific processing steps applied, change detection results at the park and local scales, and validation of the results.

TABLE OF CONTENTS

Executive Summary

We created a stack of 16 growing-season Landsat satellite images from 1985-2009 covering Ivvavik National Park and nearby Herschel Island. Four indices (NDVI, and Tasseled Cap Brightness, Greenness, and Wetness) derived from Landsat's optical channels were analyzed for per-pixel linear trends using robust regression. Trends were then summarized for both park-specific ecosystem types and general land cover classes to reveal any consistent patterns. The indices were further related to long-term change in fractional shrub and other vegetation covers using a regression tree classifier trained with 4 m resolution land cover. The results suggest a trend towards greening and fractional shrub increase in Ivvavik's coastal plain and nearby Herschel Island. These changes are corroborated by field observations of increased vascular vegetation cover and also coincide with a 1985-2009 winter warming trend. Coastal erosion and thaw slumps mapped in published studies and observed in aerial photos could also be clearly identified using the Tasseled Cap Brightness index.

1. Description of Park Vegetation

There are three main vegetation types in Ivvavik: arctic tundra, alpine tundra and taiga. Arctic and alpine tundra are the most common. Taiga is the transition between boreal forest and tundra. It consists of open stands of stunted spruce and balsam poplar. These trees grow to within 30 kilometers of the Beaufort Sea and represent the northernmost extension of their range in Canada.

Depth of permafrost and availability of moisture both affect the distribution of plants in the northern Yukon. Day length, air and soil temperature, exposure to wind, and snow conditions also have an impact on how and where plants grow. In the Firth River valley, the more delicate flowering plants as well as stands of stunted trees grow on south-facing mountain slopes and stream banks. These areas are protected and receive plenty of direct sunlight. As a result, permafrost is lower in the soil. The Malcolm and Babbage river valleys are strongly influenced by Beaufort Sea weather: frequent fog, cool temperatures and steady winds. Typical vegetation of these valleys includes tundra grasses, sedges, herbs and low shrubs.

On the coastal plain, with its proximity to the ocean, permafrost is close to the surface and precludes the growth of trees and many other plant species. The tallest plants here are willows that grow along the ground. Polygon wetlands are filled with arctic grasses, rushes and sedges. High-centred polygons, hillsides and ridges are covered with blueberries, cranberries and cloudberries. Wildflowers bloom throughout the park with the peak of colour occurring from late June through early July. Blooming is delayed in places where snow lingers (e.g. on the coastal plain) or has accumulated (e.g. along river banks or on the leeside of hills).
(from http://www.pc.gc.ca/pn-np/yt/ivvavik/natcul/natcul1.aspx)

2. Input Satellite Imagery

a) Landsat Satellite Data for Trend Analysis

Twenty-six Landsat scenes were selected primarily from WRS frames 67/11 and 68/11, which provided the greatest coverage of the park (figure 1). These were supplemented by four, high-quality no-cost scenes from 66/11 and 69/11 overlapping a smaller area of the park. Together, these frames cover > 90% of the park, with only a small gap in the southerly-most portion. Of the 26 processed scenes, we used a subset of the best 16 after examining annual phenology trends (next section) and image quality in terms of atmosphere and snow contamination (table 1).

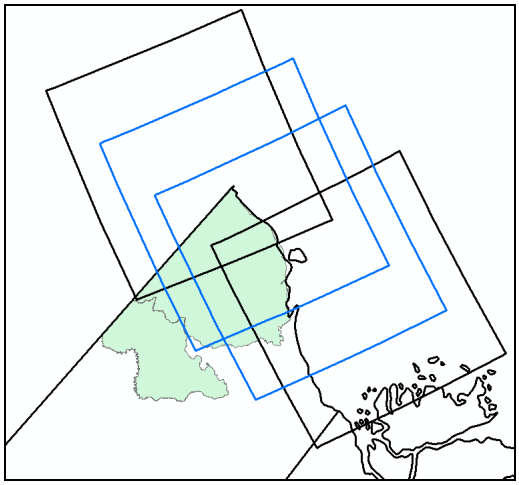

Figure 1 – Park coverage provided by WRS frames 67/11 and 68/11 (blue) and supplementary frames 66/11 and 69/11 (black)

Table 1 - Landsat scenes selected and pre-processed by WRS path/row. The final set of 16 scenes used for trend analysis is shown in bold.

Path/Row	67/11	68/11	69/11	**66/11**
Approx Park Coverage	80%	95%	35%	40%
Date 1	**2009-08-12 (24%, L5)**			2009-08-21 (12%, L5)
Date 2		2008-08-24 (23% over wat, L7 SLC-off)		
Date 3	**2007-08-23 (0%, L5)**	2007-08-30 (0%, L5)		
Date 4		**2007-08-22 (0%, L7 SLC-off)**		
Date 5		2007-07-05 (32%, L7 SLC-off)		
Date 6		**2006-07-26 (0%, L5)**		

Date 7	**2005-07-24 (14%, L7 SLC-off)**			
Date 8		2004-08-21 (20%, L5)		
Date 9	2002-07-16 (1%, L7)			
Date 10	2001-08-30 (1%, L7)	**2001-08-21 (67%, L7)**		
Date 11		**2000-08-02 (21%, L7)**		
Date 12			**1999-07-14 (0%, L5)**	
Date 13		***1998-07-20 (0%, L5)**		
Date 14		1995-07-12 (0%, L5)		
Date 15		**1994-08-10 (0%, L5)**		**1994-07-27 (0%, L5)**
Date 16	***1993-07-15 (0%, L5)**			
Date 17	**1992-07-28 (70%, L5)**	*1992-08-20 (0%, L5)		**1992-08-06 (10%, L5)**
Date 18				
Date 19	1986-07-12 (0%, L5)	**1986-08-04 (20%, L5)**		
Date 20		**1985-08-01 (20%, L5)**		

USGS Glovis http://glovis.usgs.gov/
*CCRS CEOCat3 – purchased from MDA

b) Analysis of Phenology in Landsat Time Series

Section 3-a-iii of the Protocol document describes a method that uses NDVI from AVHRR to assess how vegetation phenology at a given Landsat acquisition date compares to peak phenology for the same year. This can be used to flag scenes that deviate significantly from peak phenology and determine if there is any temporal trend in this deviation that could potentially produce a spurious change result.

Figure 2 below shows a mask of green targets in Ivvavik from which average 10-day NDVI values from 1985-present were extracted. The mean 10-day NDVI of these pixels corresponding to each Landsat acquisition date is compared to the peak 10-day NDVI for that year in figure 3. The red arrows indicate scenes that were not considered in the final trend analysis based on an assessment of this deviation and quality of each candidate image. Figure 4 shows the percent deviation from peak NDVI for the final Landsat scenes selected for trend analysis. NDVI deviation is less than three percent for all dates except two, and there is a weak, but non-significant ($p>0.05$) positive trend. Note that the impact of this trend, if any, would be to attenuate the signal from any long-term increase in vegetation greenness or cover.

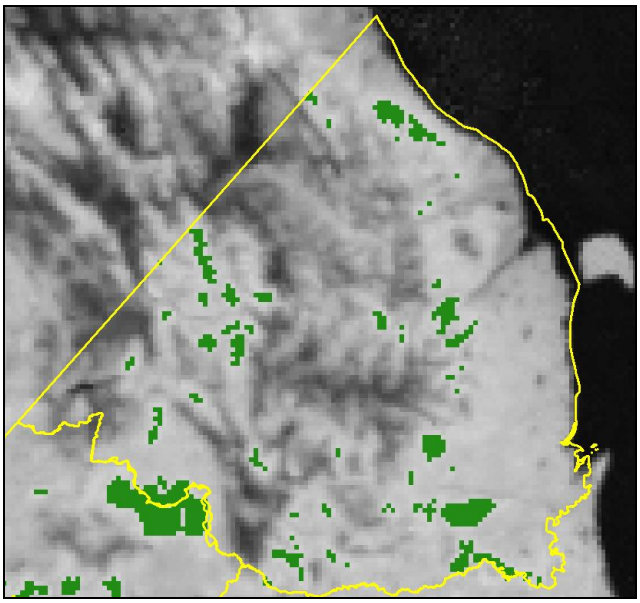

Figure 2 – Mask of green targets within Ivvavik based on multi-year growing season NDVI (mean plus one standard deviation)

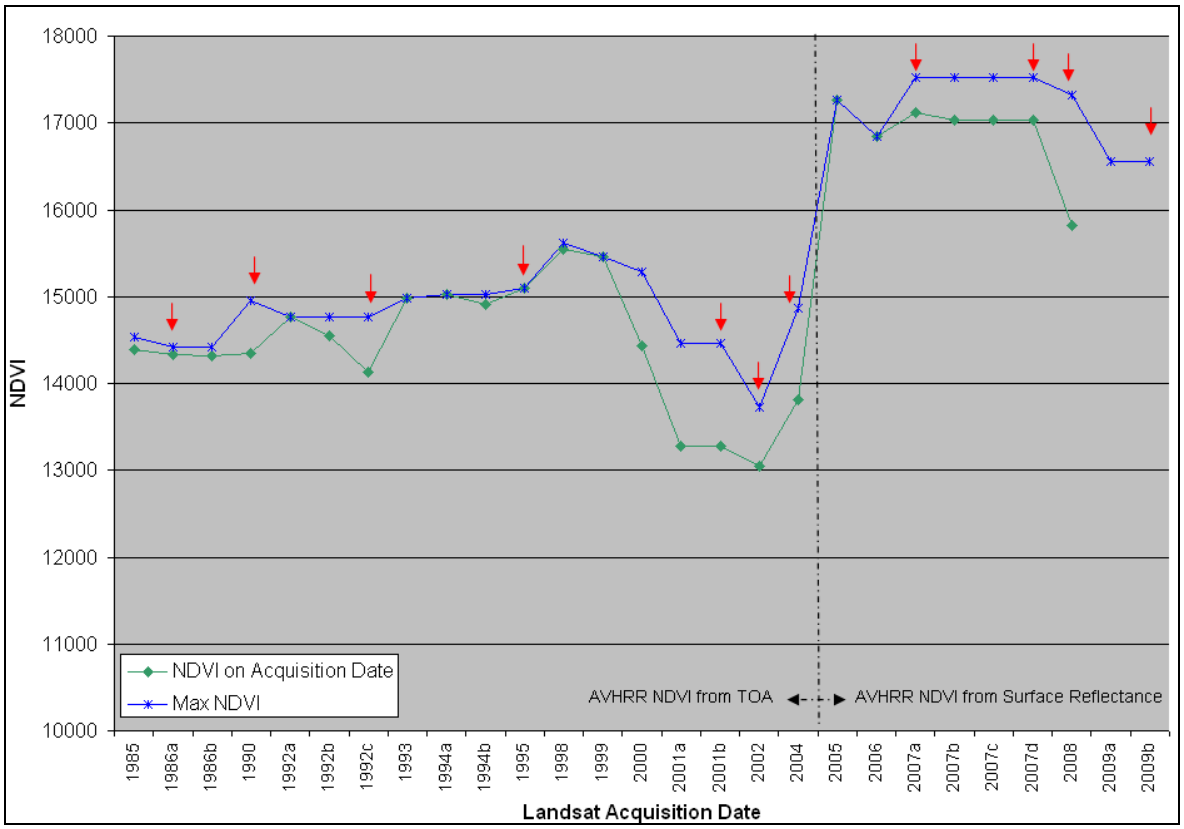

Figure 3 – Comparison of average NDVI values for each Landsat acquisition date and peak NDVI values for corresponding year, averaged over green targets within the park. Images not considered for trend analysis are indicated using the red arrows. AVHRR-NDVI data were not available for 2009.

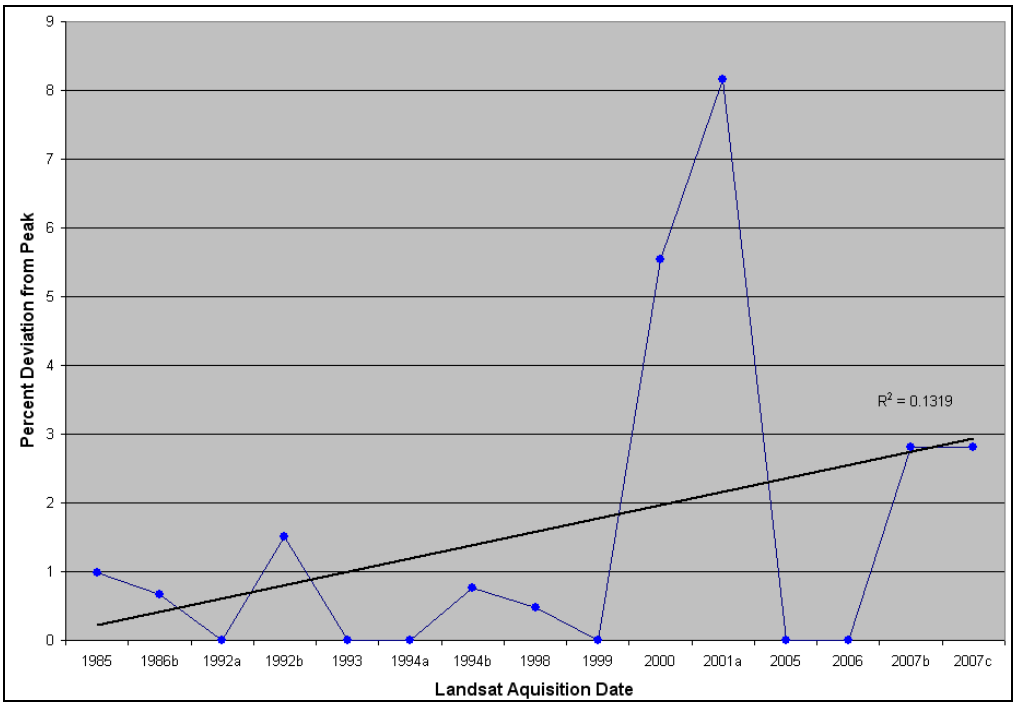

Figure 4 – Percent deviation from peak NDVI for final Landsat scenes used for trend analysis.

c) High Resolution Imagery for Upscaling Land Cover Fractions

Three high resolution scenes were acquired for Ivvavik, covering the coastal plain and foothill regions. Two were 2.4m multispectral QuickBird images from July 14, 2005 and August 9, 2006, and the other was a 4m multispectral IKONOS image from August 4, 2004. (figure 5) (for specifications see http://www.digitalglobe.com/index.php/48/Products?product_id=1 and http://www.satimagingcorp.com/satellite-sensors/ikonos.html)

All three scenes were co-registered to a baseline Landsat image using PCI's Autosync package, clustered to 60 spectral classes using ISOCLUSTER, then clusters labeled as shrub, herbaceous, water, or bare. The high resolution land cover products were then upscaled to 30m resolution using the procedure described in Section 5-b-iii of the Protocol for use as training data for the regression tree classifier.

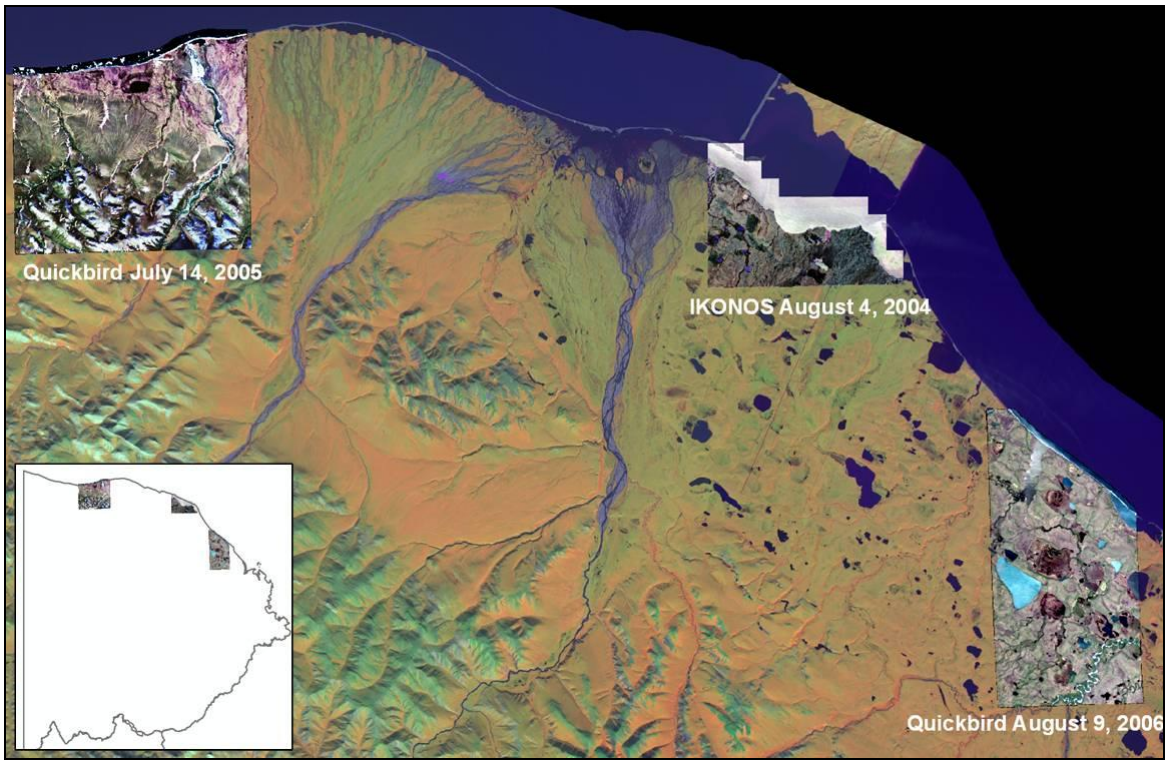

Figure 5 – Location of three high resolution scenes covering Ivvavik. Scenes are superimposed over a SPOT HRVIR image mosaic.

3. Reference Data

a) Vegetation Surveys and Maps

i) Plot surveys from a 2008 field campaign

A field sampling program, led by Parks Canada, was conducted in Ivvavik during July 14-28, 2008. The major objective was to collect vegetation information to support terrestrial ecosystem inventory and monitoring using different remote sensing tools at a range of scales.

Over 400 field sample plots were visited, where mean percent cover of major ground and vegetation growth forms (shrub, lichen, moss, herbaceous), ecotype, and digital photos were recorded. In about 80 of the sites, additional information was collected on species presence, and site and soil conditions. Unfortunately, the available high resolution scenes do not overlap with the locations of any of the field plots (figure 6).

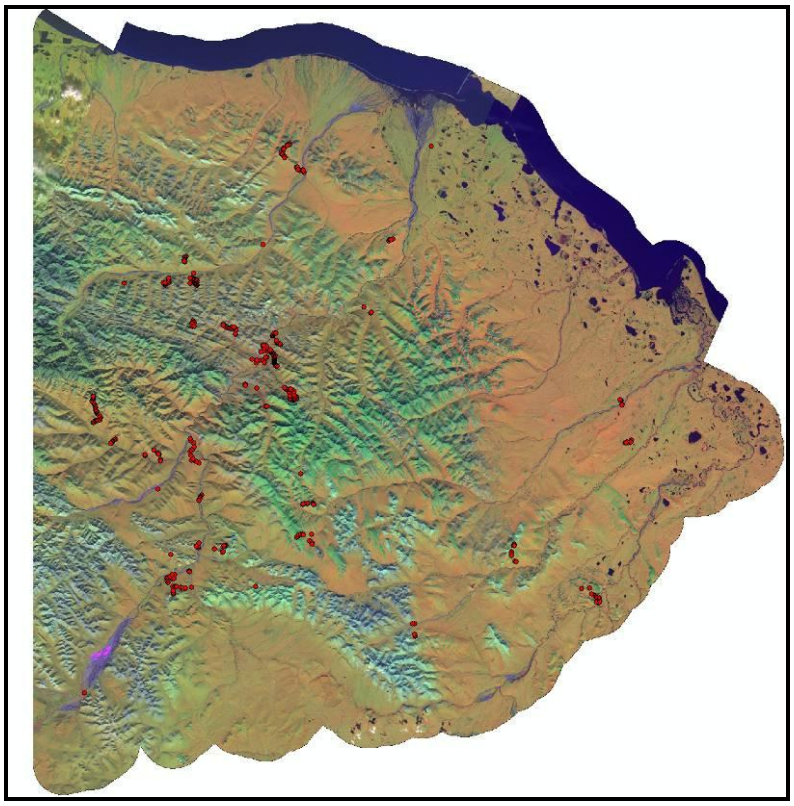

Figure 6 - Distribution of 1998 field sample sites in Ivvavik (red) superimposed over SPOT HRVIR image mosaic.

ii) Ecosystem Maps

Fraser et al. (2010) developed a method for predictive ecosystem mapping in arctic environments that integrates direct measurements from satellite remote sensing with terrain variables from a DEM representing environmental gradients related to ecotype distribution. This Image-based Predictive Ecosystem Map (I-PEM) method was applied to create a map of 28 ecotypes over Ivvavik (figure 7).

Training data for an ecotype decision tree classifier were derived from an existing 3,010 km^2 terrestrial ecosystem map (TEM) running north-south along the Firth River corridor and covering 30% of the park. This TEM was created as part of a grizzly bear habitat study and is based on interpretation of 1:20 000 scale color aerial photography. The classifier could then be applied over the entire park where 10-m SPOT HRVIR imagery and terrain parameters from DEMs were available. The PEM map reproduced the TEM classes in a hold-out testing sample with 85% accuracy.

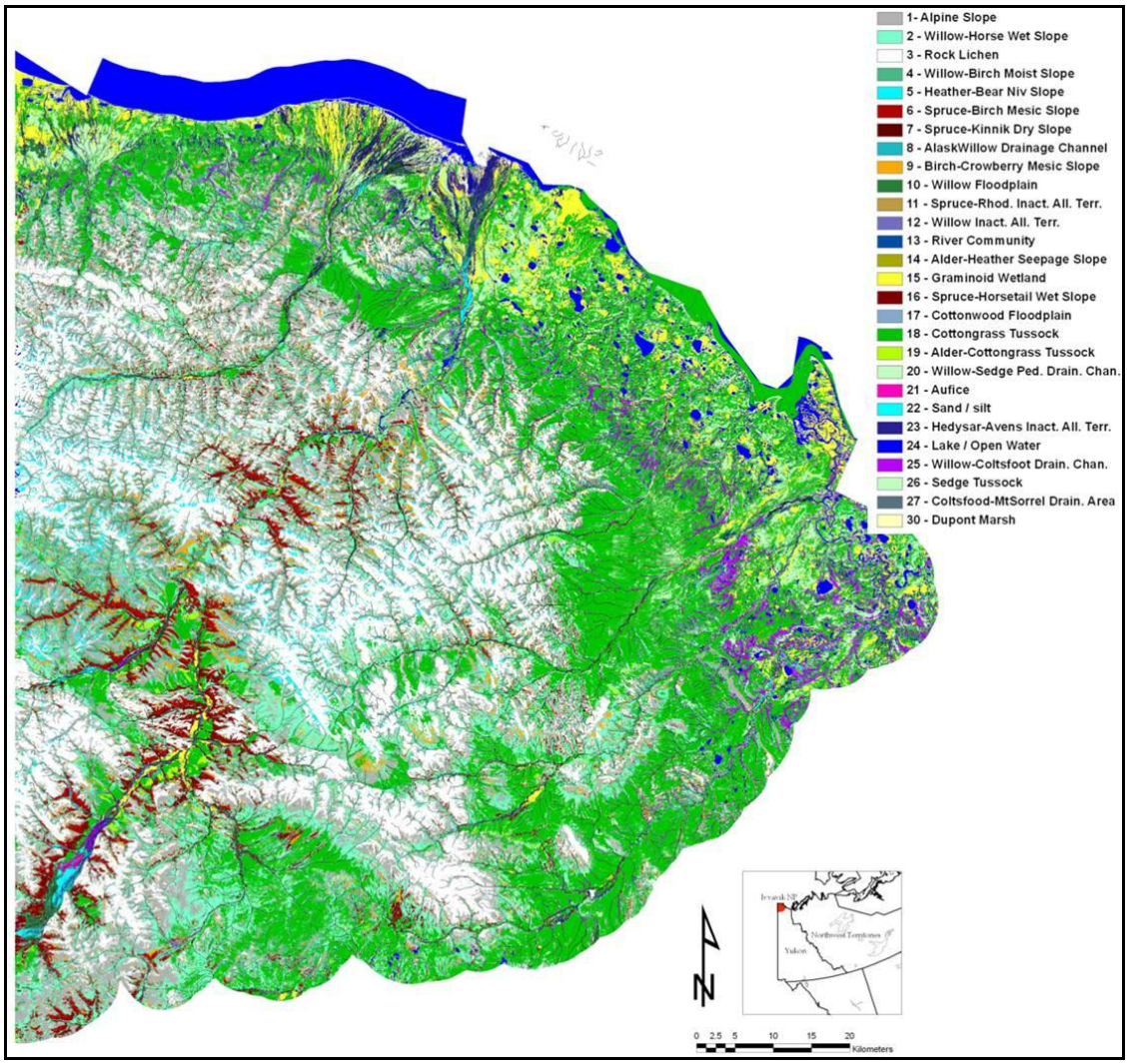

Figure 7 – 28-class PEM map for Ivvavik National Park.

iii) Land Cover Map

A 30m resolution land cover map of northern Canada was developed by Olthof et al. (2009) for application in northern land use planning, wildlife habitat assessment, and climate change impact assessment and adaptation.

Orthorectified circa 2000 Landsat data were acquired from the Centre for Topographic Information, with coverage from the treeline to the northern tip of Ellesmere Island, and combined into 16 radiometrically balanced large-area mosaics. A stratified unsupervised cluster labeling approach was used for map generation. Literature on northern land cover and vegetation mapping and numerous northern vegetation surveys were examined to define a land cover legend containing 15 classes.

Field data gathered during several campaigns were used in conjunction with other available medium-resolution land cover maps to develop a dataset for training and

validation. Standardized accuracy assessment is limited due to the cost of field data acquisition and the small archive of reference data in northern regions. Comparison with field data used only to aid cluster labeling suggests 81.5% accuracy for 76 plots, and examination of subpixel land cover distribution within each 1 km Circumpolar Arctic Vegetation Map (CAVM) class shows good agreement. The map is available through the Natural Resources Canada Geogratis portal in 1:250 000 scale National Topographic System (NTS) map sheets.

This land cover map was used to statistically summarize the Landsat-based trend and fractional change results (figure 8).

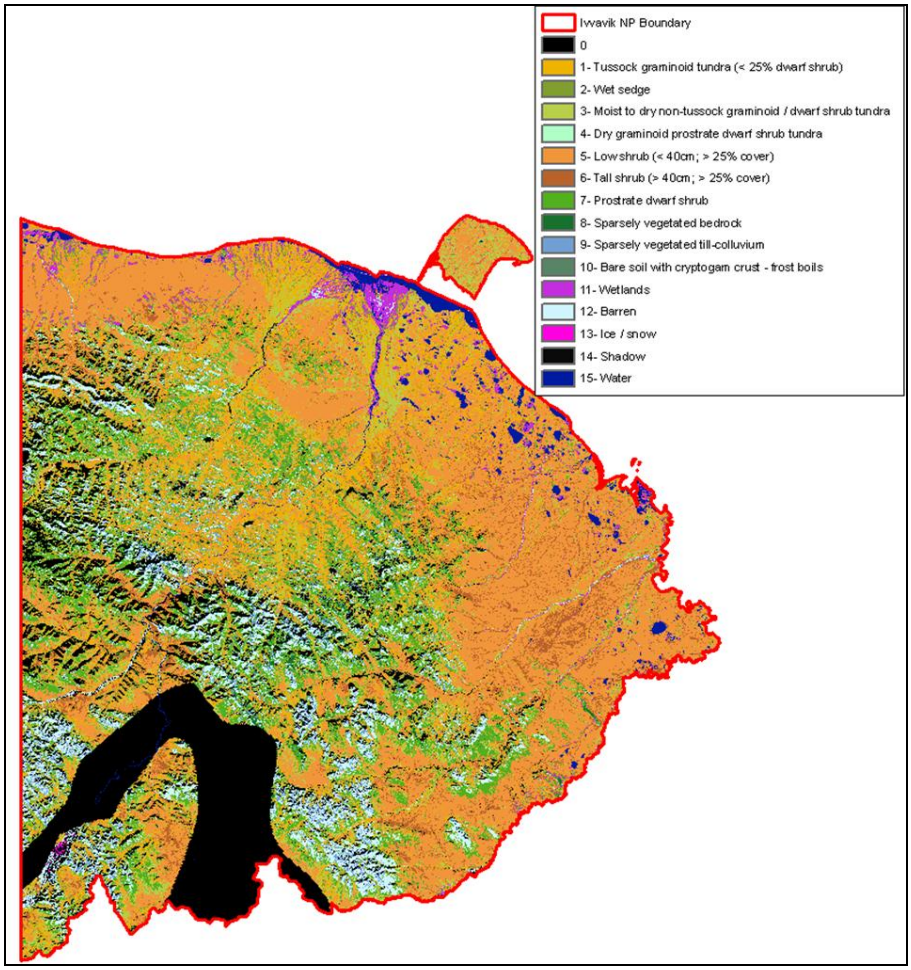

Figure 8 – 15-class land cover map for Ivvavik National Park. The missing area contains trees and is therefore not included in the product.

b) Aerial photographs

During the 2008 field campaign, several thousand ~5cm resolution, optical photos were captured by helicopter along the coastal plain and coastline. After geo-referencing and

mosaicing (figure 9), these provide a rich source of information for visually interpreting and labeling the high-resolution satellite images acquired over the same areas.

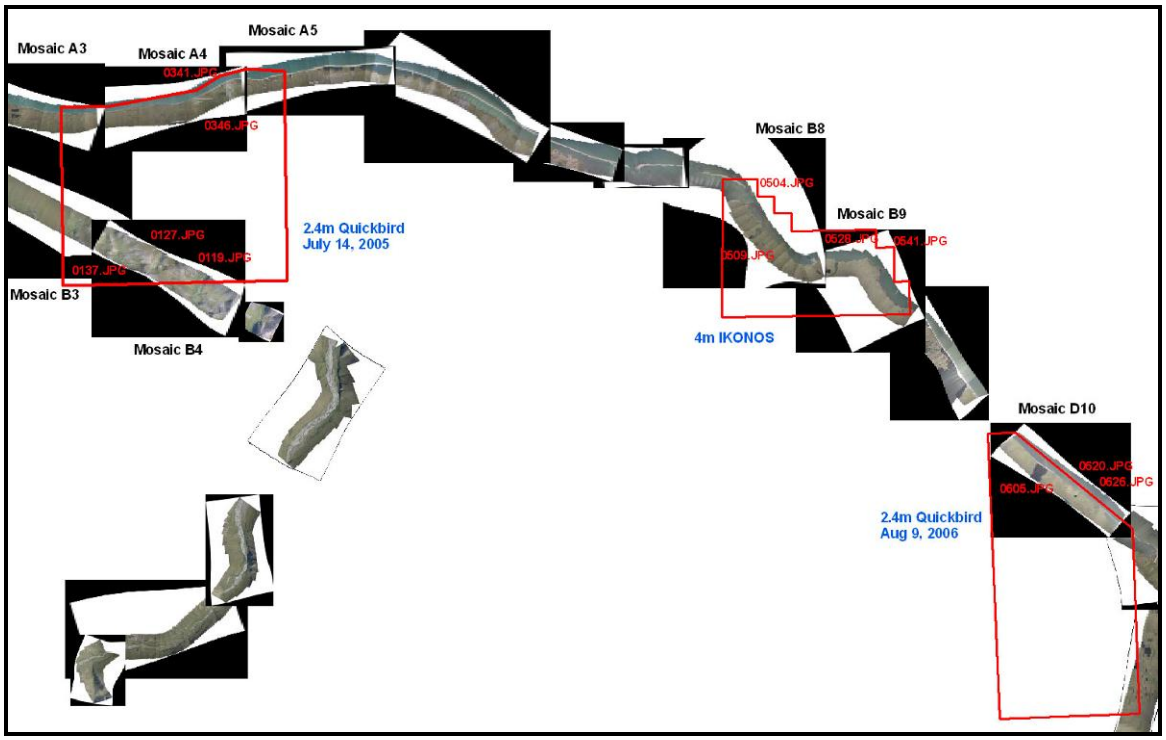

Figure 9 – Mosaiced aerial photos acquired in 2008 and coverage provided over the three high-resolution satellite images in Ivvavik's coastal plain.

c) Other spatial data

i) DEM from Yukon Environment

A set of high-quality, artifact-free digital elevation models was produced by the Government of Yukon, Department of Environment. The 30m DEMs were created using the ANUDEM program by interpolating contours and drainage from planimetrically corrected 1:50,000 NTDB map sheets. We reprojected and mosaiced the DEMs covering Ivvavik (figure 10), and also derived a suite of terrain parameters for use in PEM mapping, including slope, aspect, soil wetness index, and solar insolation.

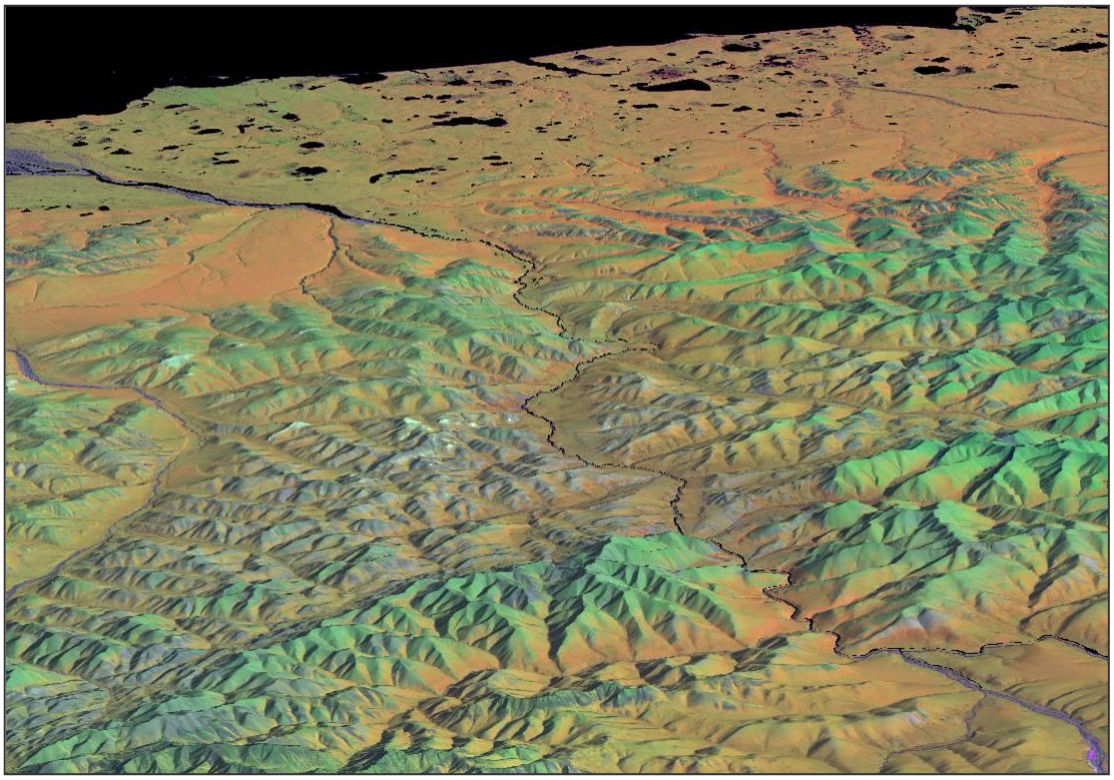

Figure 10 – SPOT HRVIR image mosaic draped over DEM for the Firth River corridor of Ivvavik.

4. Unique Landsat Processing Steps

This section describes any unique processing steps that were applied in relation to the Landsat processing methods from Section 5 of the Protocol document. It also provides results obtained for intermediate products.

As described in Section 2 above, our original selection of 26 Landsat scenes was reduced to 16 for use in trend analysis after assessing their quality and removing several that deviated significantly from peak-phenology.

We also computed a channel indicating the number of clear observations for each pixel (figure 11) (Section 5-b-ii of the Protocol). This was used to exclude areas from analysis that had few observations ($n<6$) and where the computed trends may be unreliable.

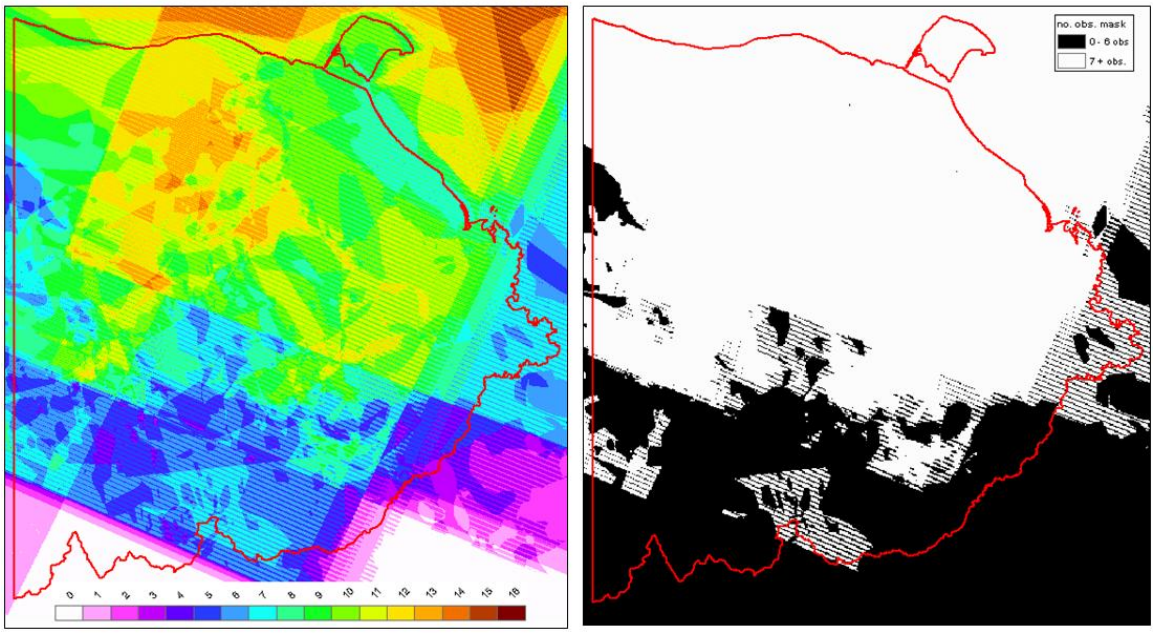

Figure 11 – Number of clear-sky observations channel (left) and bitmap showing areas with six or more observations used in trend analysis (right).

In examining the initial trend results, we observed that less illuminated north-east facing slopes demonstrate large spectral changes through the time series, often resulting in false trends. This is due to large changes in solar illumination occurring over these areas throughout the summer. For example, figure 12 shows negative NDVI trends in red overlaid on a shaded DEM relief for a mountainous portion of Ivvavik, where the low-illumination NE slopes appear dark.

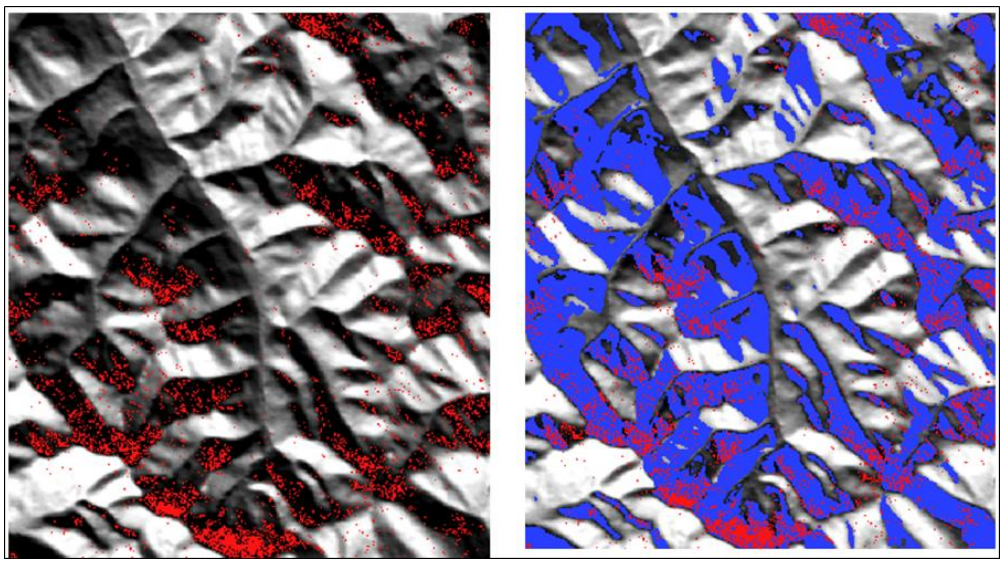
Figure 12 – Left shows negative NDVI trends in red superimposed over hillshaded DEM in a mountainous portion of Ivvavik. The right panel shows that a mask identifying steep, NE facing slopes (blue) are able to flag these areas.

We therefore used a combination of slope and aspect to create a mask that identified steep slopes receiving low solar radiation (figure 13). Slope was calculated as percent rise, and aspect can be thought of as the slope direction expressed in degrees from 0 to 360, measured clockwise from north. A transformation of aspect was derived where the most illuminated SW slopes are given a value 0, increasing to a value of 200 for the least illuminated NE slopes. A combined mask was created that identifies steep slopes (i.e. > 30 percent) facing north of NW or NE.

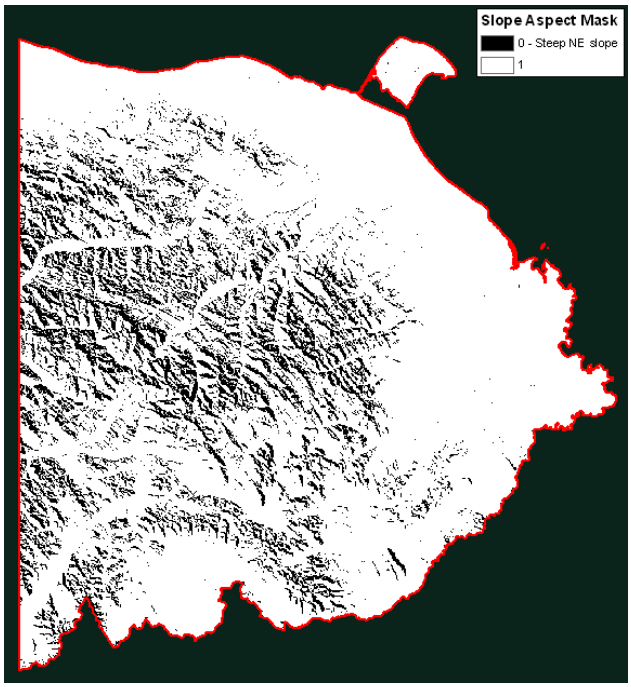

Figure 13 – Slope-aspect mask (black) used for Ivvavik to exclude areas of high insolation variability from trend analysis.

5. Trend Analysis Results and Derived EI Measures

a) Trends in Vegetation Indices (VI)

i) Park-wide VI trends

Grayscale images showing the temporal trend (i.e., regression slope) for the four vegetation indices (NDVI, and Tasseled Cap Greenness, Wetness, and Brightness) are shown in the left panels below. Bright pixels (positive values) represent areas of increasing slope while the dark pixels (negative values) represent areas of decreasing slope. The right panels show only those pixels where slope is significant at $p<0.05$. Areas of positive slope are shown in green and areas of negative slope in red.

NDVI demonstrated a significantly positive trend over 5.6 percent of the Landsat analysis window (figure 14). Positive trends occurred mainly on portions of the coastal plain and nearby Herschel Island. Only 1.2 percent of the area had a negative trend, with most of

these areas associated with higher elevations and in areas of dynamic river braiding close to the Beaufort.

Tasseled Cap Greenness (TCG) (figure 15), not surprisingly, demonstrated similar trends to NDVI. TCG significantly increased over 6.1 percent of the study area and decreased over 1.3 percent.

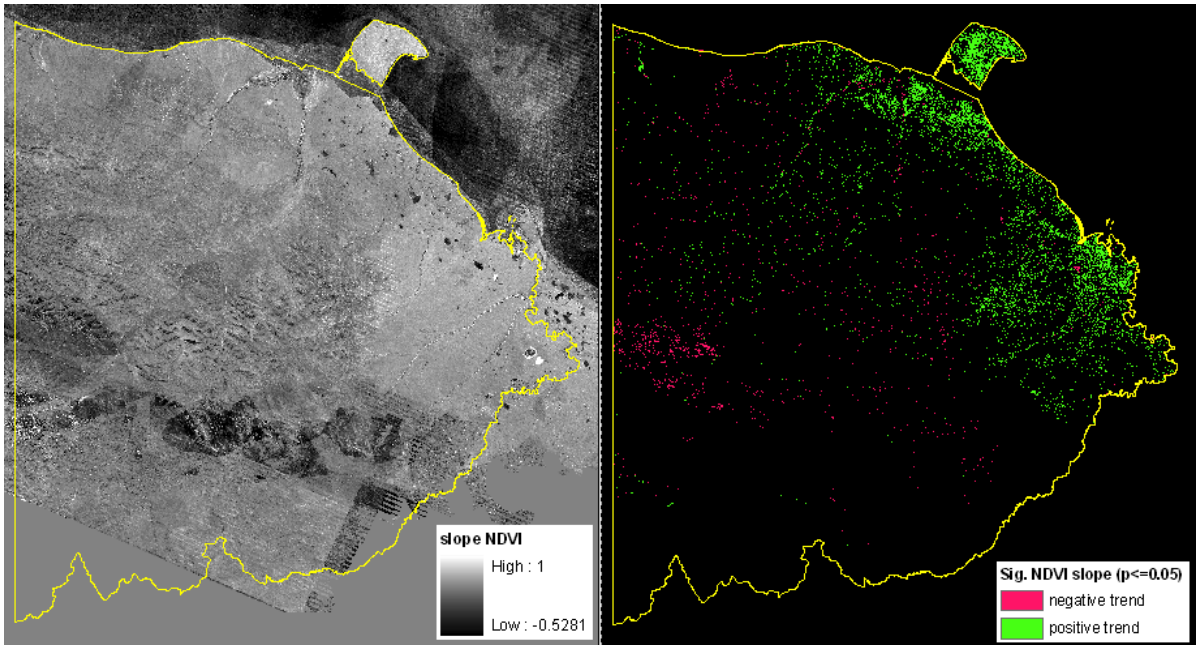

Figure 14 –NDVI slope from regression trend analysis (left), and areas having significant (p<0.05) negative and positive trends.

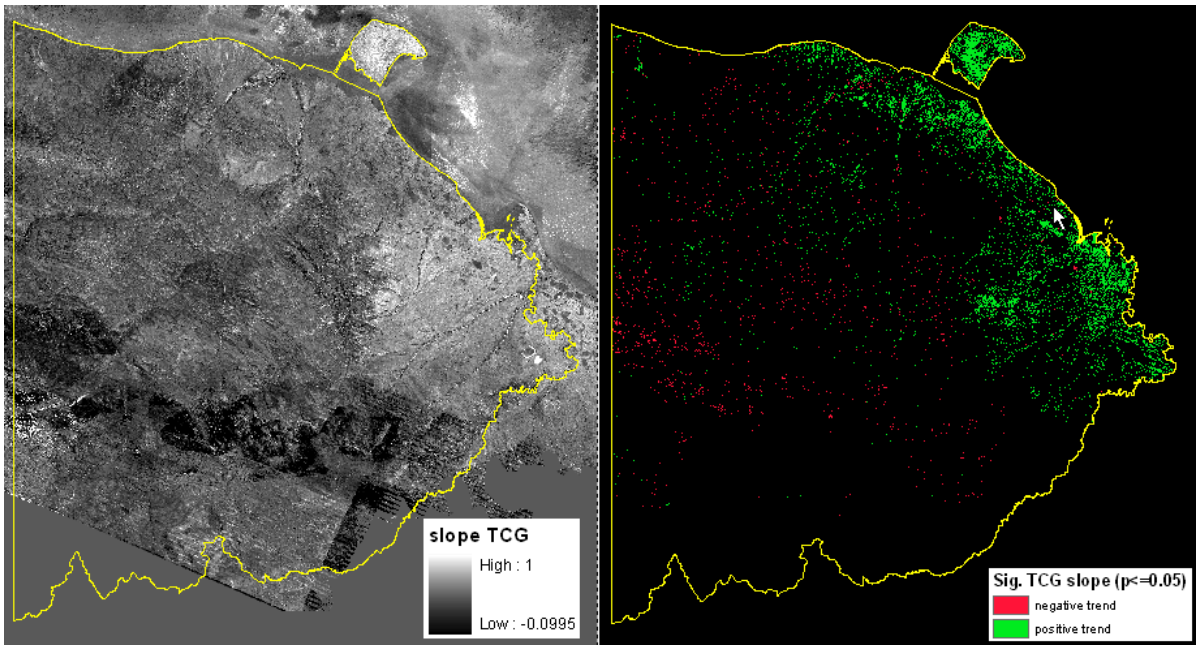

Figure 15 –TCG slope from regression trend analysis (left), and areas having significant (p<0.05) negative and positive trends.

Tasseled Cap wetness (TCW), measuring the contrast between shortwave-infrared (SWIR) and visible/ near-infrared (VNIR) reflectance, can be related to soil or surface moisture content. TCW was observed to increase over 3.1 percent of the park and decrease over 9.6% of the area (figure 16). Negative trends were especially associated with south and westerly facing slopes in the mountains (figure 17).

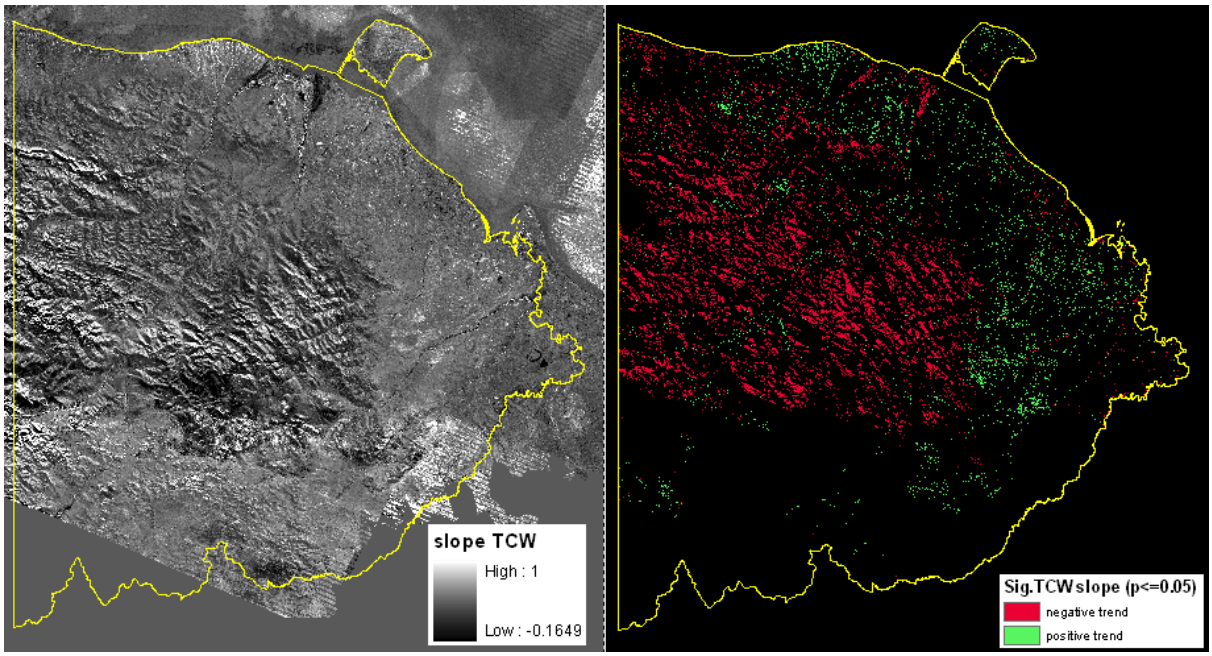

Figure 16 –TCW slope from regression trend analysis (left), and areas having significant ($p<0.05$) negative and positive trends.

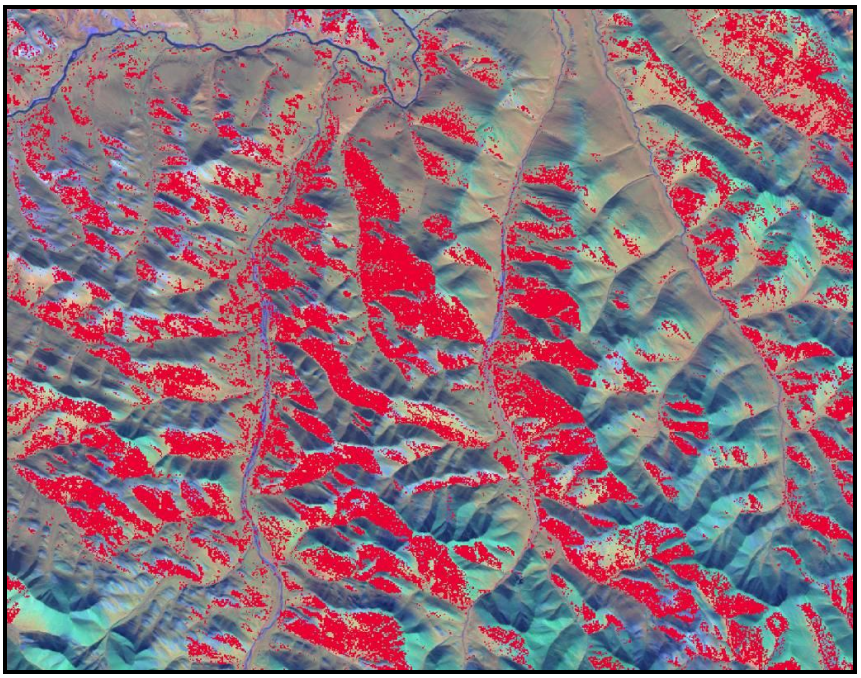
Figure 17 – Close-up of negative TCW slopes overlaid on SPOT image, showing that they are often associated with south or west facing slopes.

The most widespread trends were observed in the Tasseled Cap Brightness index (TCB), which decreased over 17.3 percent and increased over 1.3 percent of the study area (figure 18). TCB is a weighted sum of all six Landsat optical bands, and provides a measure of overall reflectance that is able to separate light from dark soils or vegetation from bare areas. Many riparian areas in the park, both on the coastal plain (Fig 19a) and in the mountains (Fig 19b), show a negative TCB trend. Since these areas typically contain willow and/or alder shrubs, a decreasing brightness would be consistent with increased growth of shrub vegetation and shadowing over a lighter soil or rock background (Stow and others, 1993).

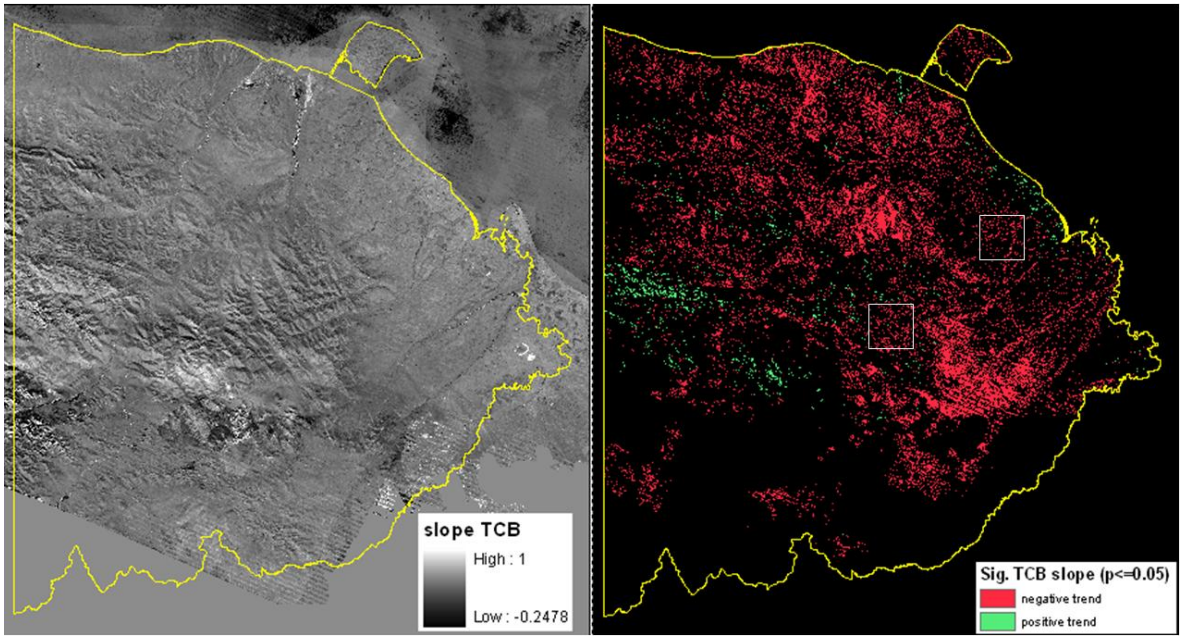

Figure 18 –TCB slope from regression trend analysis (left), and areas having significant ($p<0.05$) negative and positive trends.

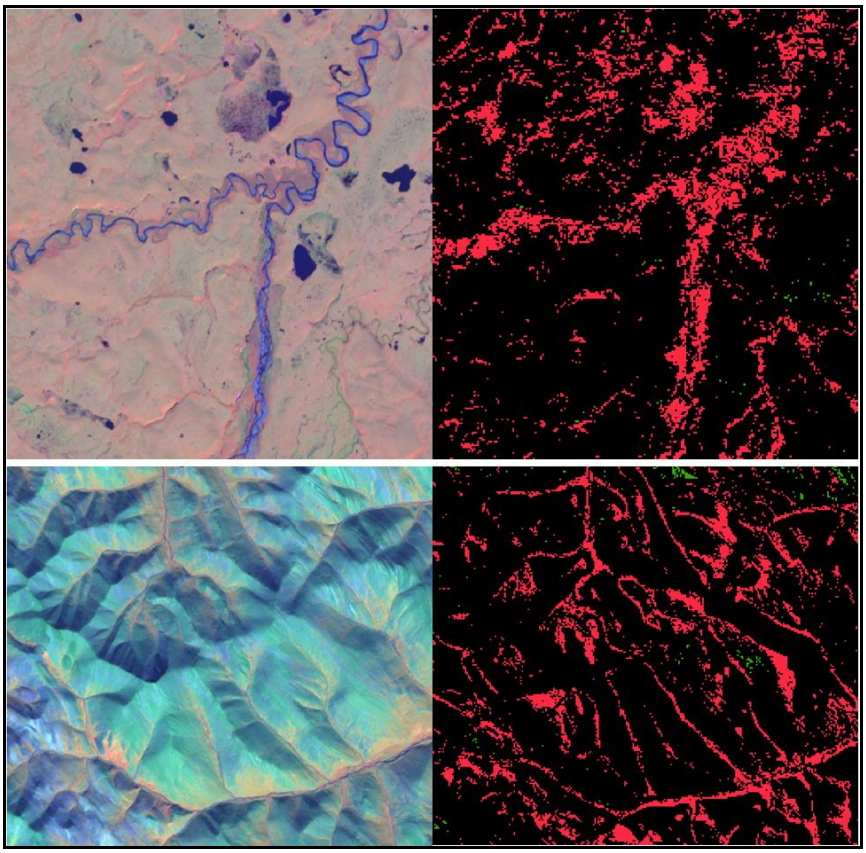

Figure 19 – Close-up of SPOT image mosaic and negative TCB slopes for riparian areas on the coastal plain (top) and mountains (bottom). Locations are indicated in figure 18.

Close-up figure of the TC index trends were also created for the area surrounding the warden station at Sheep Creek, just upstream from the Firth River (figure 20). This area is of particular interest because of number of available field measurements collected by Parks Canada. The major trends within in this area were decreasing brightness, especially associated with ecotypes containing spruce and willow, and decreasing wetness on southwesterly-facing slopes. Again, a darker surface would be consistent with increased growth in tall shrub and spruce vegetation.

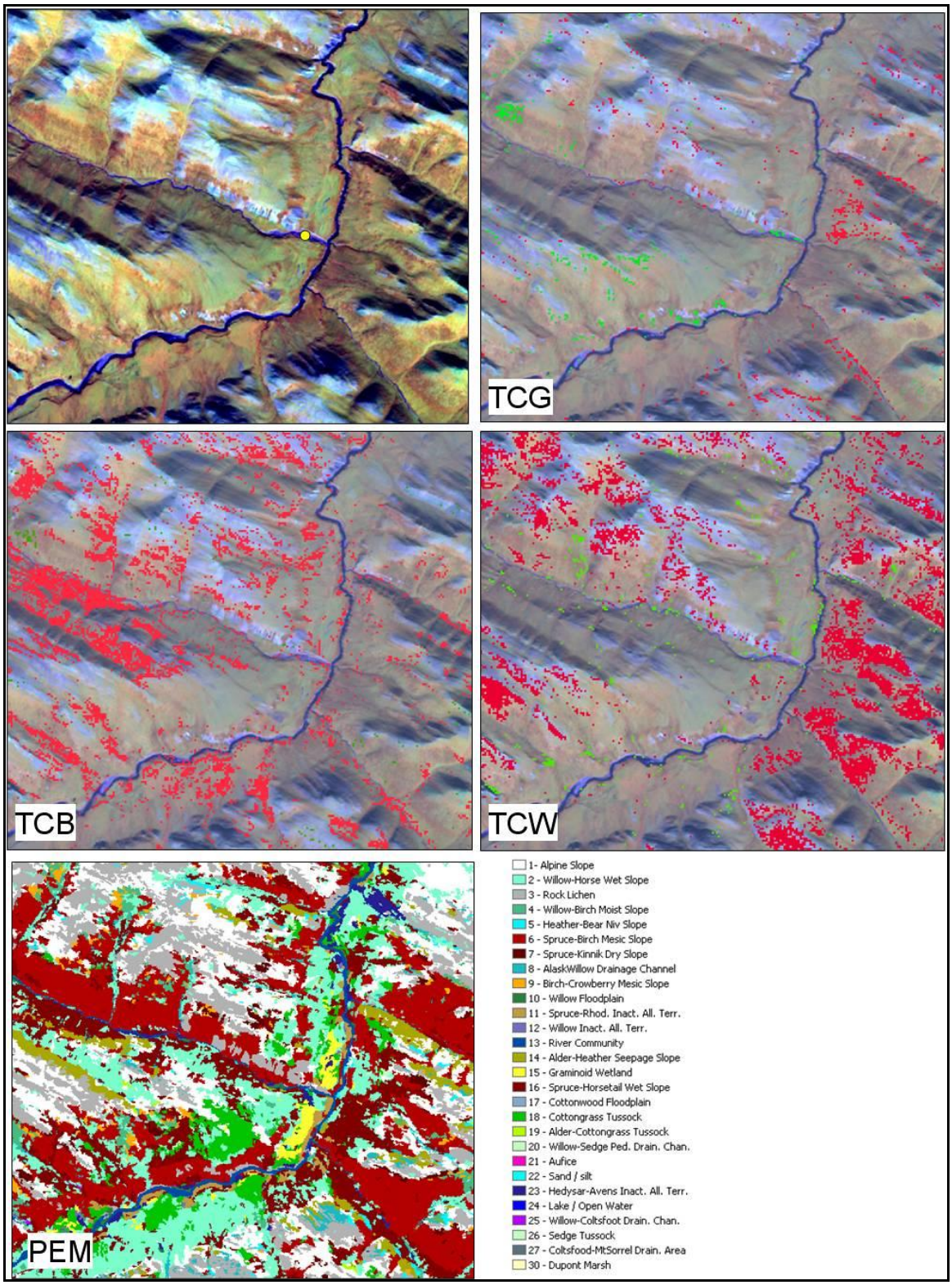

Figure 20 – 7-by-6 km area around the Sheep Creek Warden Station showing the SPOT image (station location in yellow), three Tasseled Cap indices, and PEM map.

ii) VI Trends by Land Cover and Ecotype

The vegetation index (VI) trends can also be summarized by land cover and ecosystem class to better understand which vegetation types are exhibiting the largest changes. Ecosystem or vegetation-specific trends can also be rolled-up to provide EI Measures for reporting on Indicators, which Parks Canada defines as high-level ecosystem types, such as tundra and wetlands. For this, we use both the Predictive Ecosystem Map (PEM) and land cover classification described in Section 3-A.

The average trend or slope for each VI is summarized graphically for the PEM ecotypes (figure 21) and northern land cover classes (figure 22). Most of the NDVI and TCG trends are similar, with a general positive (greening-up) trend in the coastal plain land covers and ecotypes and little change or small decreases in vegetation types at higher elevations. A general trend towards declining TCB is found across most land covers and ecotypes. TCW shows a similar, but less pronounced widespread drop, except in some coastal ecotypes dominated by graminoids, which show a small positive trend.

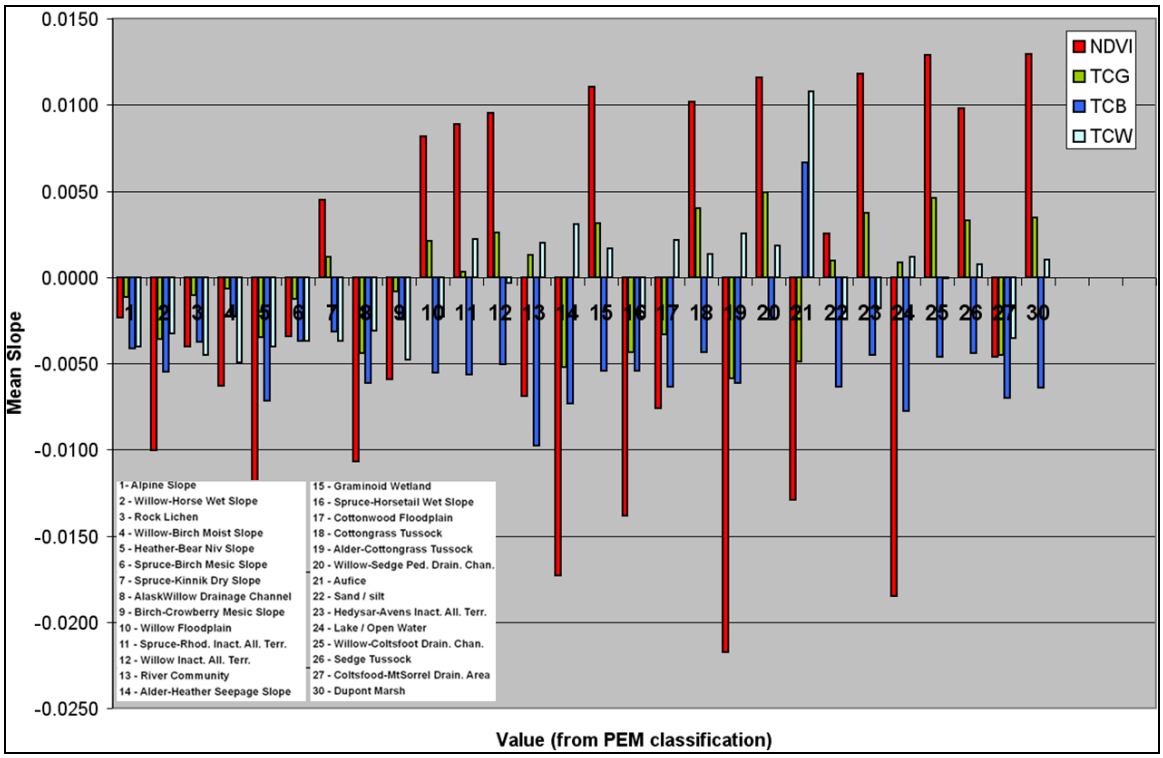

Figure 21: Chart showing the mean slope value for each class value in the Predictive Ecosystem Mapping (PEM) classification.

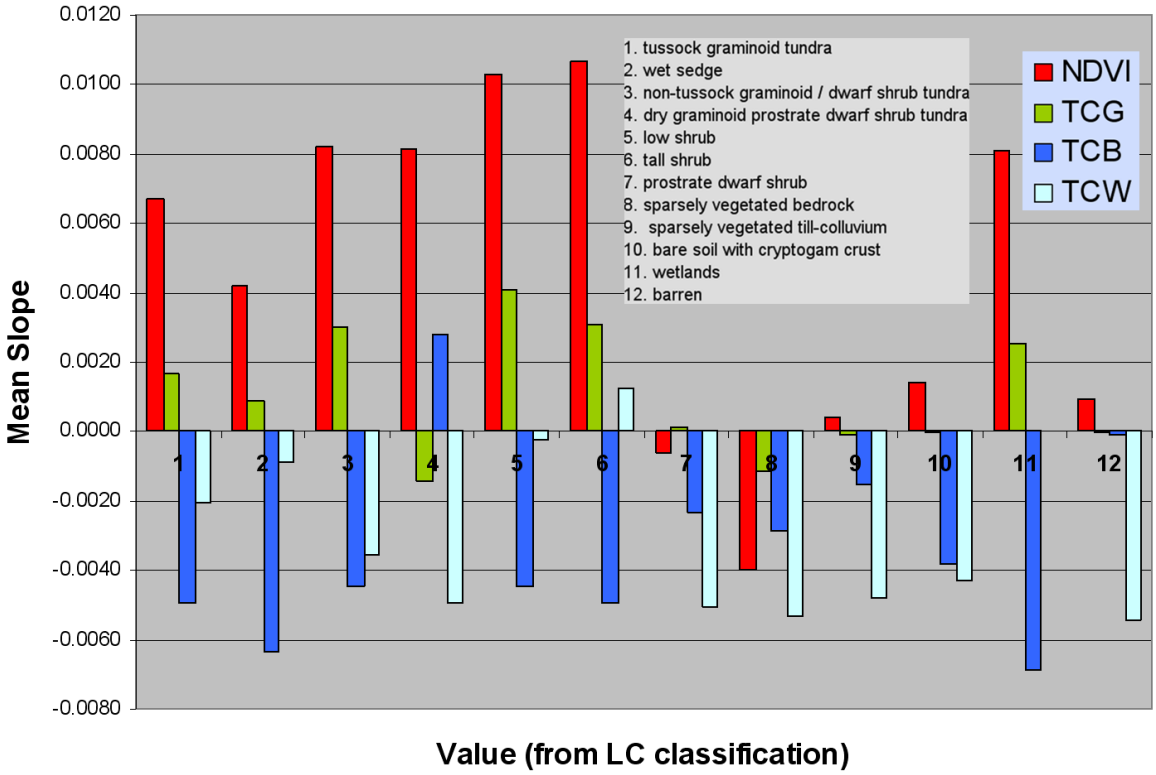

Figure 22: Chart showing the mean slope value for each class value in the Northern Land classification

b) Trends in Sub-pixel Land Cover Fractions

i) Regression Tree Models

Section 5-b-iii of the Protocol document describes how to convert the long-term Landsat VI trends into a quantitative estimate of how basic land cover proportions are changing within each pixel. This is accomplished by calculating "true" 30 m land cover fractions for a training dataset based on spatially aggregating a high resolution land cover product. For Ivvavik, we used the 4 m resolution IKONOS scene, as this provided the best shrub fraction samples from the three high resolution scenes. After the training dataset was prepared, it was used to construct Cubist regression tree (RT) models for shrub, herbaceous, bare, and water fractions. RT models were then applied for the first and last Landsat acquisition dates to create 1985-2009 fraction change maps.

The approach for extracting TC index values for training and applying the RT is illustrated in figure 23. The Cubist regression tree package by Rulequest Research was used to construct trees to predict the 30 m fractions for each class based on the three TC regression trend values corresponding to the Ikonos date. Trees could then be applied to the TC regression trend values derived for 1985 and 2009. In cases where pixels did not display significant ($p<0.05$) trends in a given TC index, the mean TC value from all pixel-level observations in the Landsat stack was used and held constant. A simple

differencing of fractions from 1985 and 2009 quantified the changes predicted during the Landsat observation period.

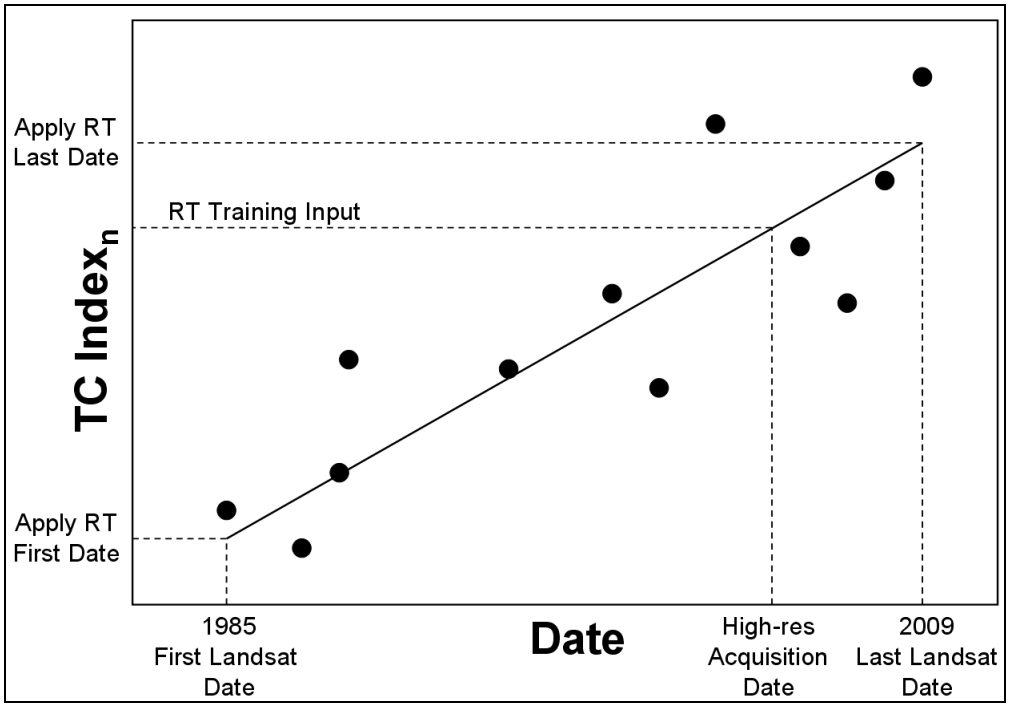

Figure 23: Approaches for training and applying regression tree models to calculate change fractions

Figure 24 shows accuracy plots for the regression tree models for shrub, herb, moss, bare, and water fractions, which were evaluated on the holdout 30% testing dataset. Comparing the estimated and calculated 30 m fractions, average absolute errors ranged from 0.7-3.8% and correlations coefficients (r) ranged from 0.79-0.95. Overall, these model results are superior to those obtained by Olthof and Fraser (2007) for mapping Landsat fractions in other areas of northern Canada.

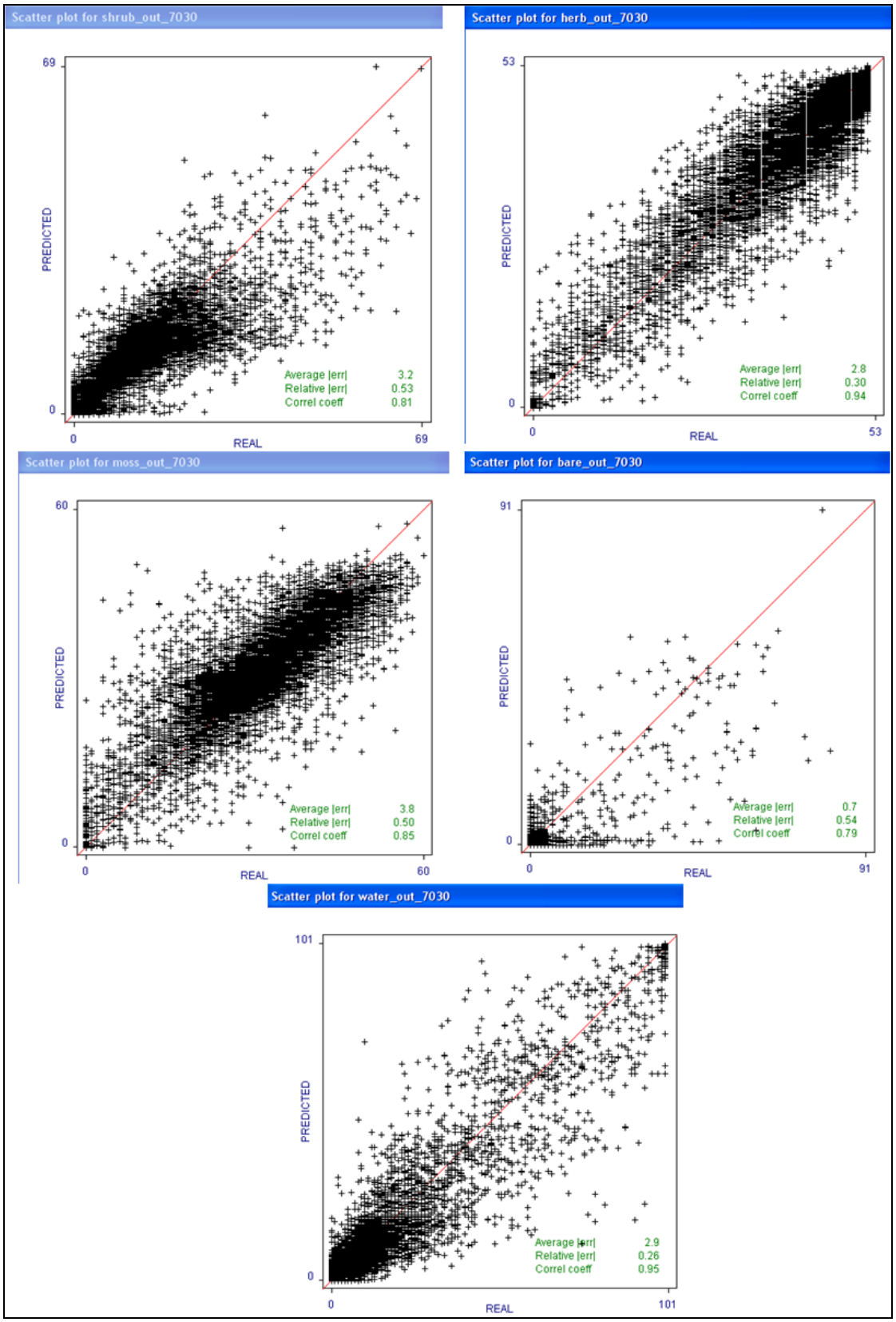

Figure 24: Regression tree accuracy assessment plots from Cubist.

ii) Park-wide fraction trends

The table below shows for each land cover fraction, the proportion of the analysis window where that fraction is decreasing, shows no change, and is increasing. Average change for each fraction is also shown.

Table 2. Summary of Landsat-based fractional changes

	%area decrease	%area no change	%area increase	average %change
bare	21.0	74.0	5.1	-1.8
herb	23.2	67.6	9.2	-1.9
moss	20.4	67.7	11.9	-1.0
shrub	6.1	70.1	23.9	3.6
water	3.9	83.1	13.0	1.1

Figure 25 displays those areas that are predicted to be increasing and decreasing in each land cover class between 1985 and 2009. Note that many areas on Herschel Island and the coastal plain demonstrating an increase in TC Greenness were also observed to have increasing shrub and herbaceous fractions, and a decreasing bare fraction. Several large patches in the mountain foothills (figure 26, centre of study area) showed a unique pattern of shrub increase with a corresponding decrease in the herbaceous and/or bare fraction. This vegetation consists of graminoid tussock mixed with varying amounts of willow and birch, and exposed rocky soil at higher elevations. Note that these patches were associated with a drop in TC Brightness but surprisingly little or no change in Greenness. This could be attributable to the lower visible reflectance of shrub compared to graminoid and bare ground (Stow and others, 1993). The net result of these spatial trends was a predicted average decrease in bare of 21%, balanced by an increase in shrub of 23.9% over the study area.

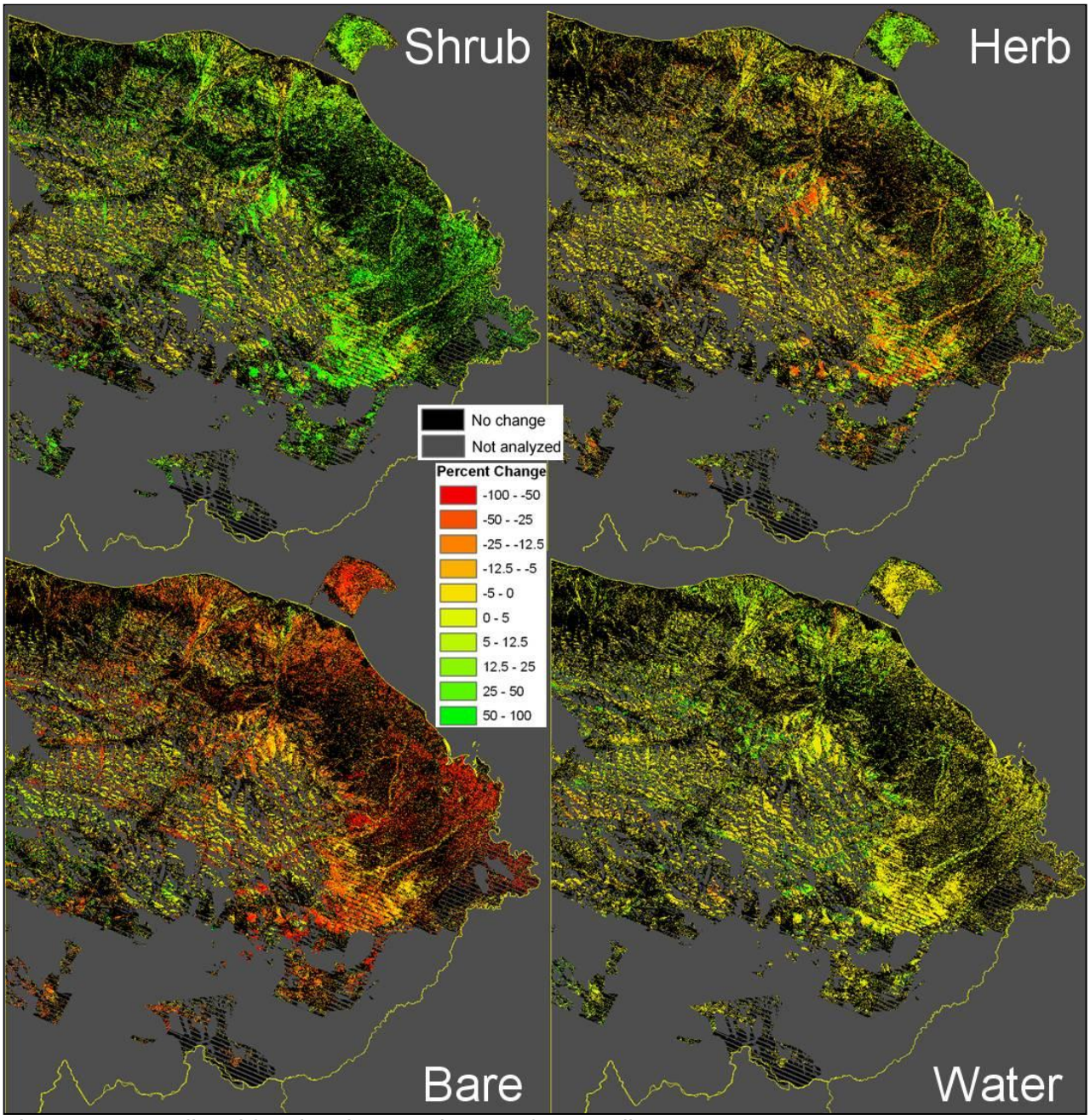

Figure 25 - Predicted fractional cover changes for Ivvavik.

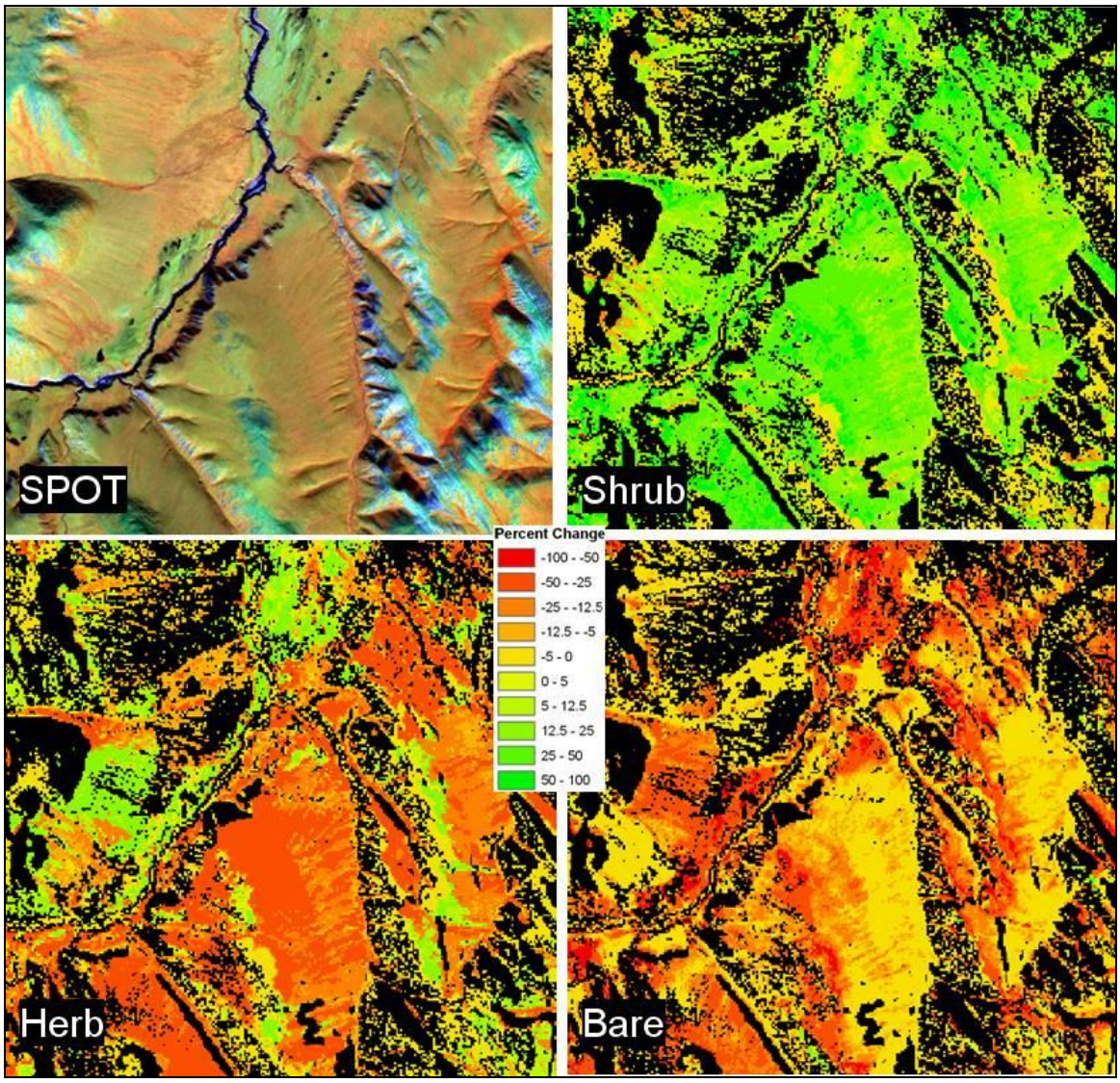

Figure 26 - Predicted fractional cover changes for foothills area in central Ivvavik.

iii) Fraction Trends by Land Cover and Ecotype

The predicted fractional changes can also be summarized by ecosystem or land cover type to better understand which vegetation types are exhibiting the largest changes. For this, the PEM ecosystem map and land cover classification product for northern Canada was used based on circa 2000 Landsat imagery (Olthof and others, 2009). The average fractional change within each ecosystem and land cover class is summarized in figures 27 and 28. The largest increases in shrub with corresponding decreases in bare and herb occurred in the higher biomass classes (i.e. land cover types 1-3, 5-6). By contrast, more sparsely vegetated classes typically located at higher elevations demonstrated limited changes in the shrub fractions. Note that these alpine communities are strongly controlled by topographic factors that limit soil development, moisture, and nutrient supply (Walker, 2000).

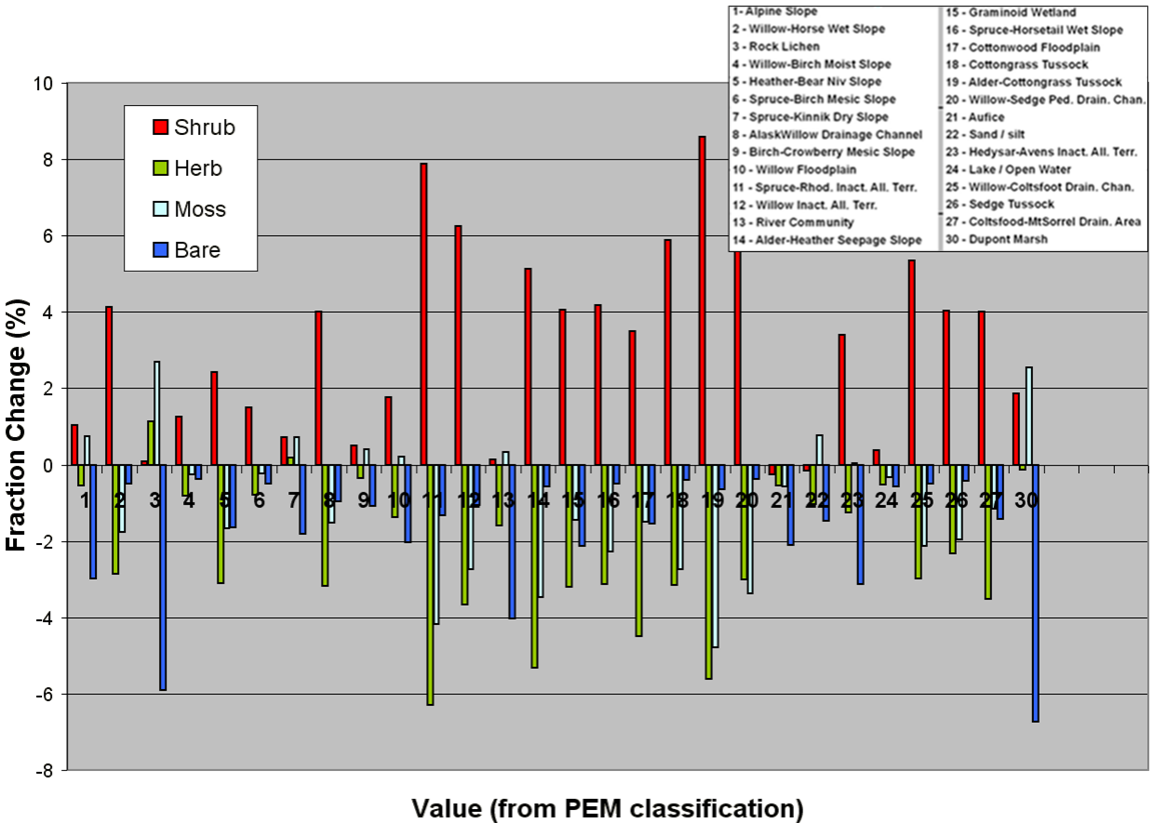

Figure 27 - Fractional vegetation changes by Ecotype.

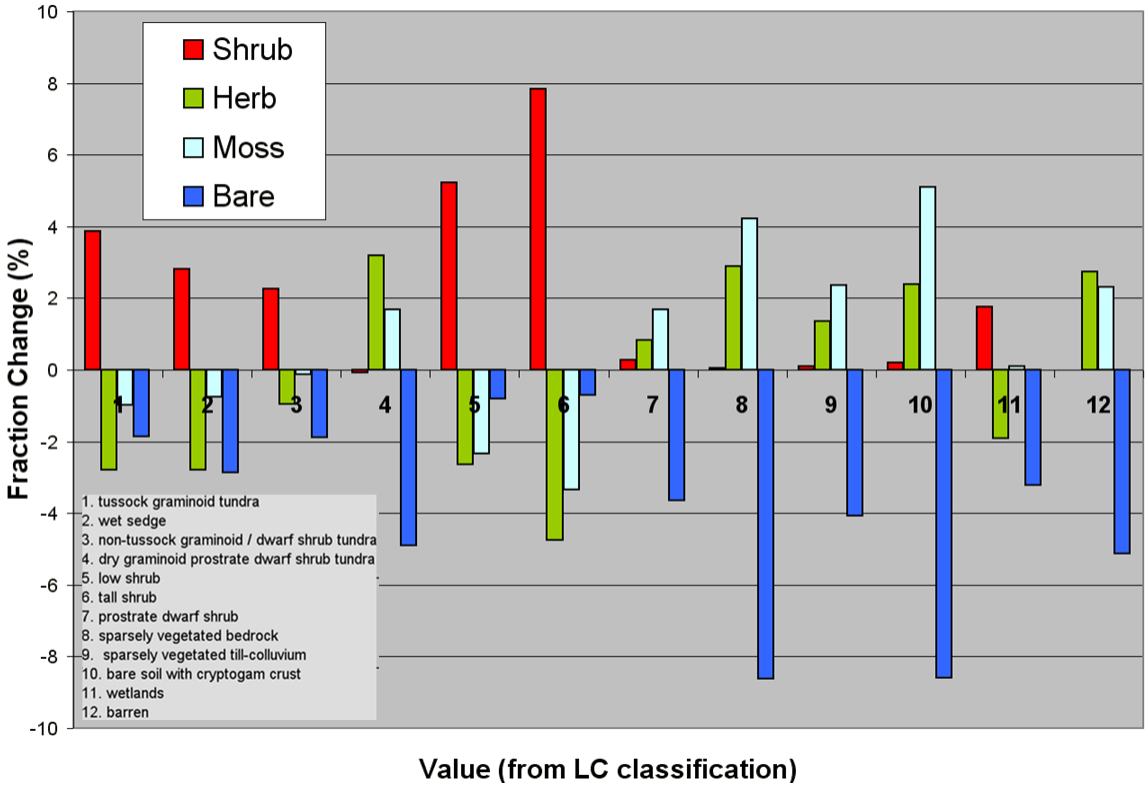

Figure 28 - Fractional vegetation changes by land cover type

c) Specific Local Trend Results and Validation

Section 3c of the Methods Protocol document provides a general discussion of validation issues related to the Landsat change detection approach. The first type of validation that can be conducted is to assess the models used to detect the trends and changes in fractional land cover. This was presented in the results sections above. Note that the summary statistics reported from the index trends were based only on pixels where TheilSen regression was significant at the 95% confidence level (i.e. $p<0.05$). Significance was tested using the rank-based non-parametric Mann-Kendall (MK) test. Additional confidence for the trend analysis comes from using a minimum of six, calibrated Landsat scenes and 10-day AVHRR-NDVI data ensure that scenes were representative of peak growing condition.

We further examined uncertainty in the trends by calculating 95% confidence limits for the NDVI Theil slope on a per pixel basis. The Kendall test statistic was used for small sample approximations where there were less than 10 observations, while the standard normal distribution was used for large sample approximations. The statistic computes the ranks of the slope values at the upper and lower confidence interval limits for the slope. The slope values at those ranks are output to the lower and upper confidence images. A one-tailed test was performed to map all areas where slopes were positive at $P > 0.975$, indicating significant greening or negative at $P < 0.975$ indicating significant NDVI decrease or browning (Kendall and Stuart, 1967). Note that the result (figure 29) closely matches the positive and negative NDVI and TCG slopes shown in figures 14 and 15.

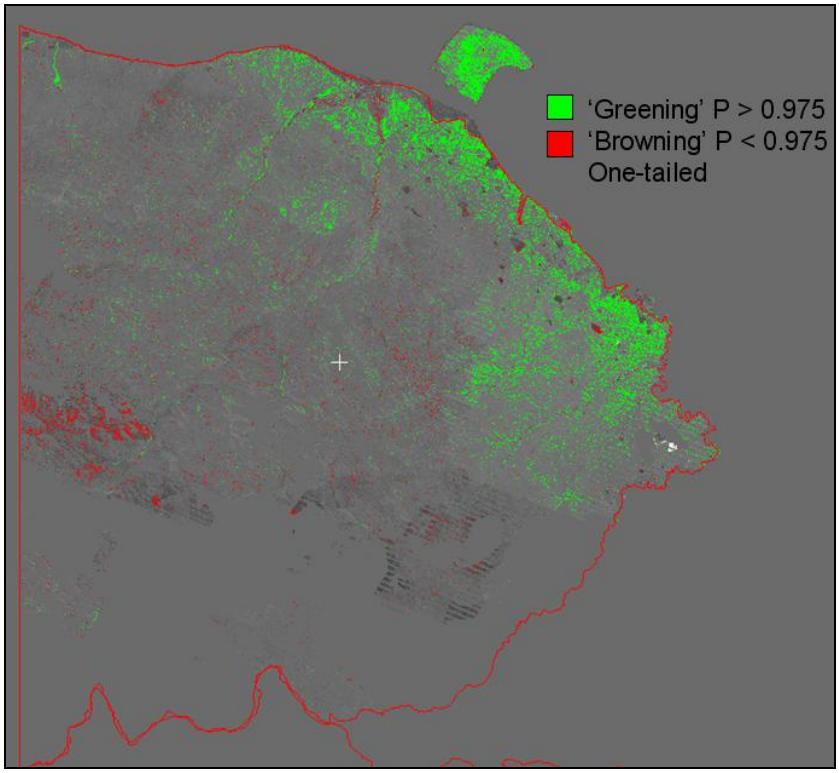

Figure 29 - Areas where the 95% confidence intervals on the NDVI slope are all either negative (red) or positive (green).

The regression tree models used for fractional land cover mapping were assessed using the standard error and correlation coefficients for a hold-out test sample. This gives an indication of the accuracy and precision of the models for the specific conditions that they were developed under. However, this represents a best-case scenario, since it assumes that errors will be comparable when applying the models over a larger area or at different time periods. Studies have demonstrated that accuracy of fractional cover estimates drops with geographical distance from the training site (Fernandes and others, 2004; Olthof and Fraser, 2007).

An independent accuracy assessment of the fractional changes is challenging owing to the lack of repeat vegetation observations—a frequent problem for Arctic change studies. One means of corroborating the trends and increasing confidence in the results is to compare them with observations from published studies or air photos documenting different types of surface changes over the Ivvavik landscape. Below we present three examples.

i) Ground-Based Vegetation Surveys

Vegetation resource inventories were conducted within the study area in 1985-1986 on Herschel Island and in 1988-1989 on Ivvavik's coastal plain (Kennedy, 2008; Kennedy personal communication). These biophysical inventories involved comprehensive surveys of vegetation, soil, and surficial geology at several hundred sites. A study was later conducted to investigate if significant vegetation changes were occurring on these sites. Subsequent field observations found that, within 12-15 years, cover of the native grass species (polargrass, Arctagrostis latifolia) had significantly increased on upland sites (figure 30). There was also an increase in low shrub and decrease in lichen and bare ground. Polargrass and Arctic lupin (L. arcticus) were also found to have increased in cottongrass tussock sites on Herschel Island but not on the coastal plain.

A more recent study on Herschel Island used historic photographs, repeat vegetation surveys, and monitoring of long-term plots to document changes in willow growth (Myers-Smith et al., 2011). This analysis suggested a recent increase in the canopy cover and height of each of the dominant canopy-forming willow species.

Overall, the results from the Landsat trend and fractional change analysis are consistent with these ground-based observations. We found that Kennedy's study area coincides with the strongest positive trends in NDVI (figure 31). On Herschel Island, estimated herbaceous land cover increased on average by 9% (figure 32), shrubs increased by 10%, and bare ground cover decreased by 21%. The trends are also directionally compatible with long-term sample plot measurements taken about 300 km to the west of the study area in the foothills of the Brooks Range in Alaska. In this moist tussock tundra site, shrub and graminoid cover increased by 60-80% from 1989 to 2008 (Gould et al., 2009).

Recent increases in Arctic shrub abundance are best explained by longer and warmer growing seasons promoting plant growth (Goetz et al., 2005; Jia et al., 2009) and increasing nutrient mineralization and availability (Chapin et al., 1995). However, in the

study region, available climate reanalysis and weather station data suggest a trend towards milder winters but little change in summer air temperatures (Section 5d). A mechanism that could permit increased shrub growth in the absence of warmer growing seasons is described in Sturm et al. (2005). They propose a positive feedback effect where shrub growth leads to locally deeper snow, which promotes higher winter soil temperatures, greater microbial activity, and more plant-available nitrogen. High levels of soil nitrogen then favour shrub growth the following summer. Note that increased winter soil temperatures and nutrient mineralization might also be expected from milder winters in northern Yukon, independent of any shrub feedback effect (e.g. Hill and Henry, 2010).

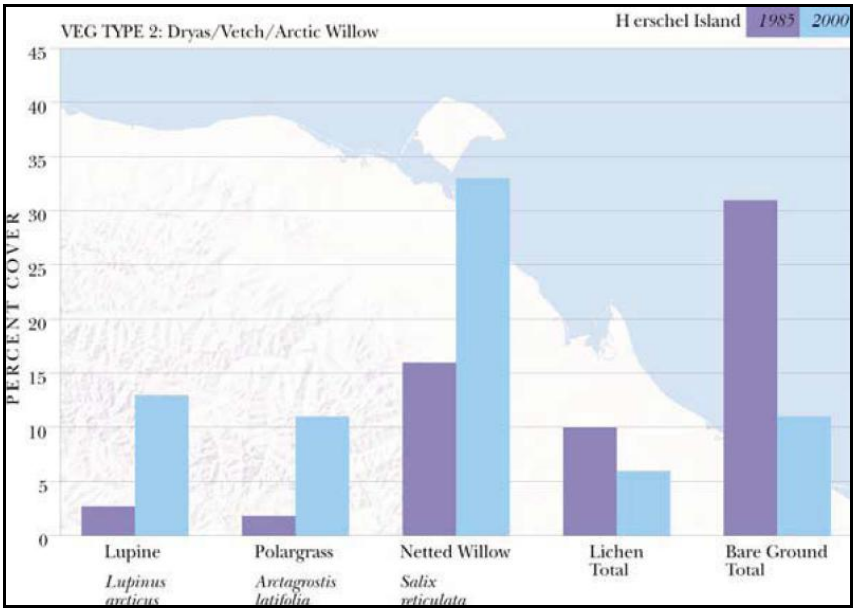

Figure 30 – Changes in percent cover observed by Kennedy in the dryas/vetch/Arctic willow tundra vegetation types. For more information see: http://www.pc.gc.ca/docs/v-g/rs-rm2002/sec3/page1.aspx and http://www.wmacns.ca/pdfs/224_2007_NSC-SummaryReport.pdf

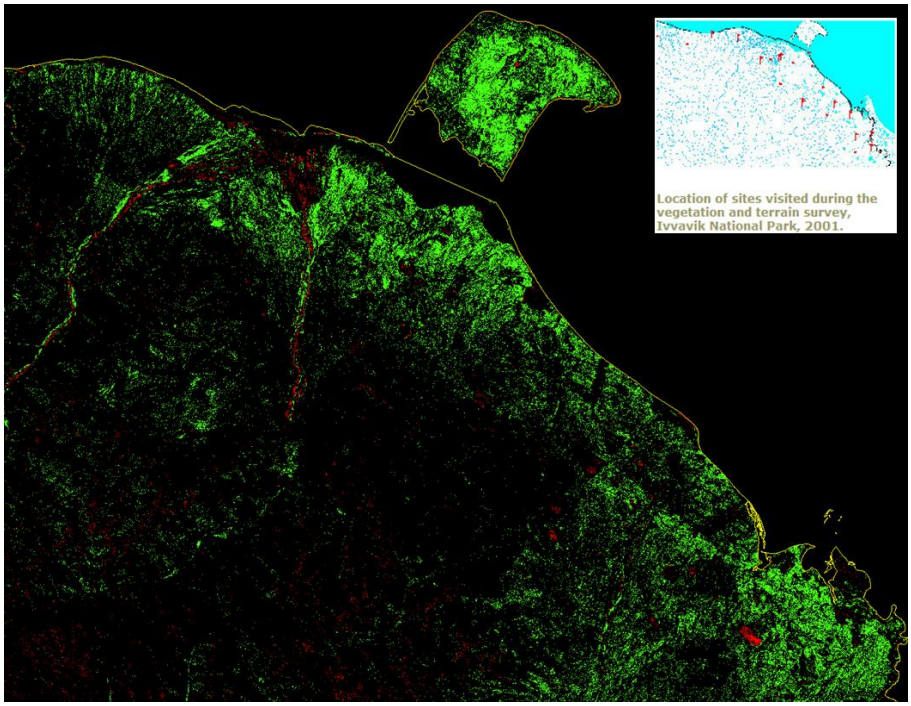

Figure 31 – Close-up of NDVI trends on Herschel Island and along the nearby coastal plain.

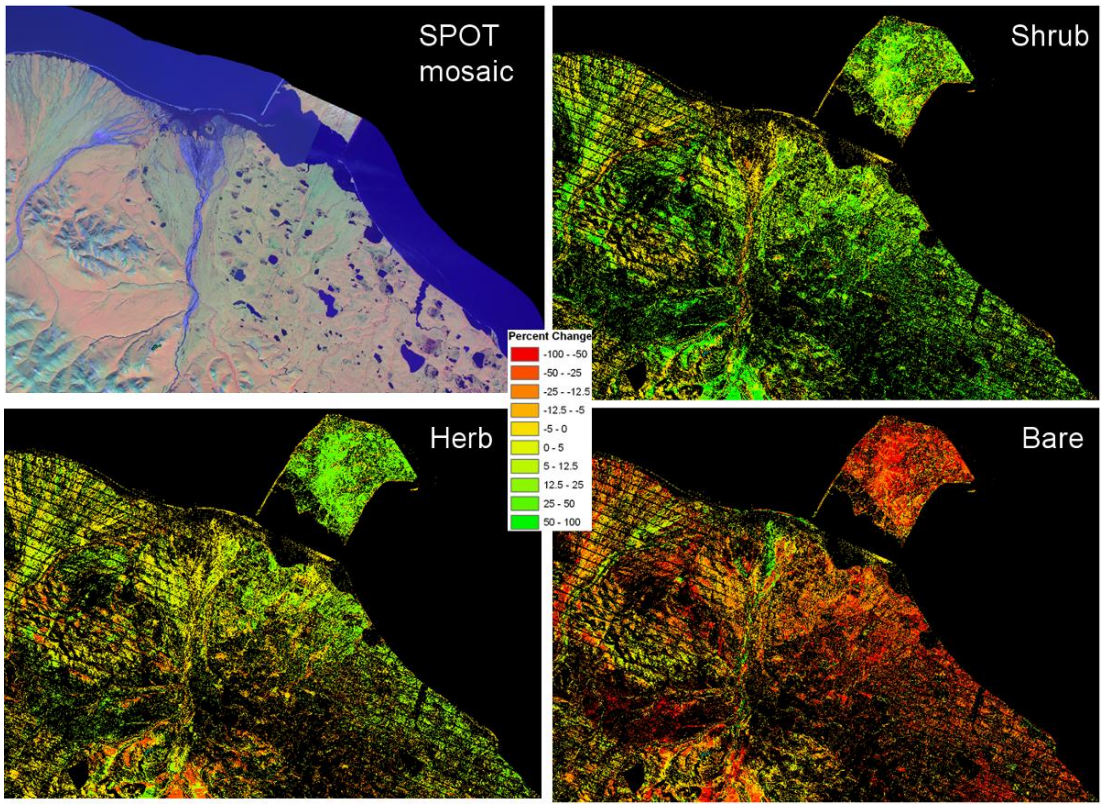

Figure 32 – Change in shrub, herbaceous, and bare fractions for Herschel Island and along the nearby coastal plain.

ii) Herschel Erosion Maps.

Herschel Island, lying north the Ivvavik coastline and within the Landsat analysis window, has been subject to high rates of coastal erosion and thaw slumping caused by melting of ice-rich permafrost. Lantuit and Pollard (2008) performed a remote sensing study on the long-term patterns of coastal erosion and retrogressive thaw slump activity for Herschel (figure 33). Using orthorectified airphotos from 1952 and 1970 and an Ikonos image from 2000, mean coastal retreat rates of 0.61 m/yr and 0.45m/yr were calculated for the periods 1952–1970 and 1970–2000, respectively. The highest coastal retreat rates were found on north–west facing shorelines, which correspond to the main direction of storm-related wave attack. During the period 1970–2000 coastal retreat rates for south to south–east facing shorelines displayed a distinct increase even though these are the most sheltered orientations. However, south to south–east facing shorelines corresponded to the orientations where the highest densities of retrogressive thaw slumps were observed (figure 34). The number and the total area of retrogressive thaw slumps increased by 125% and 160%, respectively, between 1952 and 2000 (Lantuit and Pollard, 2008).

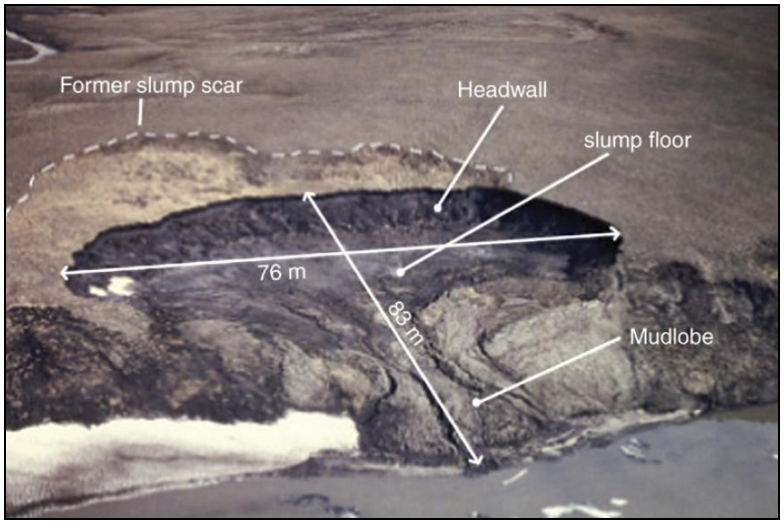

Figure 33 - Helicopter view of a polycyclic slump in Thetis Bay, Herschel Island (from Lantuit and Pollard, 2008)

Comparing Lantuit and Pollard's maps of coastal erosion rates and areas of slump activity to the Landsat trends (figure 34), we found that the TC Brightness trend was particularly sensitive to coastal erosion on Herschel, while this change was also evident as an increasing water fraction. Here, the strong declines resulted from a vegetated land surface being replaced by water or wet soil, both of which are dark surfaces.

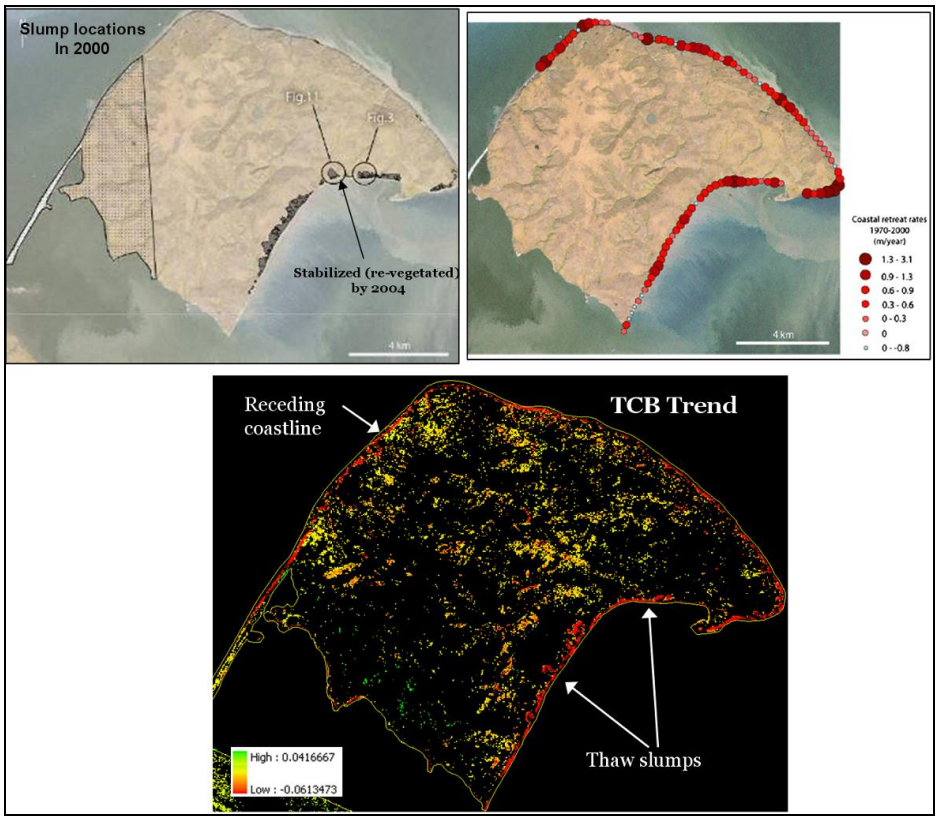

Figure 34 – Comparison of Hershel thaw slump locations (upper left) and coastal retreat rates (upper right) with TCB slope value for significant ($p<0.05$) regression trends

iii) Features Visible in Aerial Photos and Landsat image pairs

The air photos acquired in summer 2008 and described in Section 3b can be used to identify the likely cause of distinct trend features in the Landsat indices and land cover fractional products. Several examples are shown in figures 35-37.

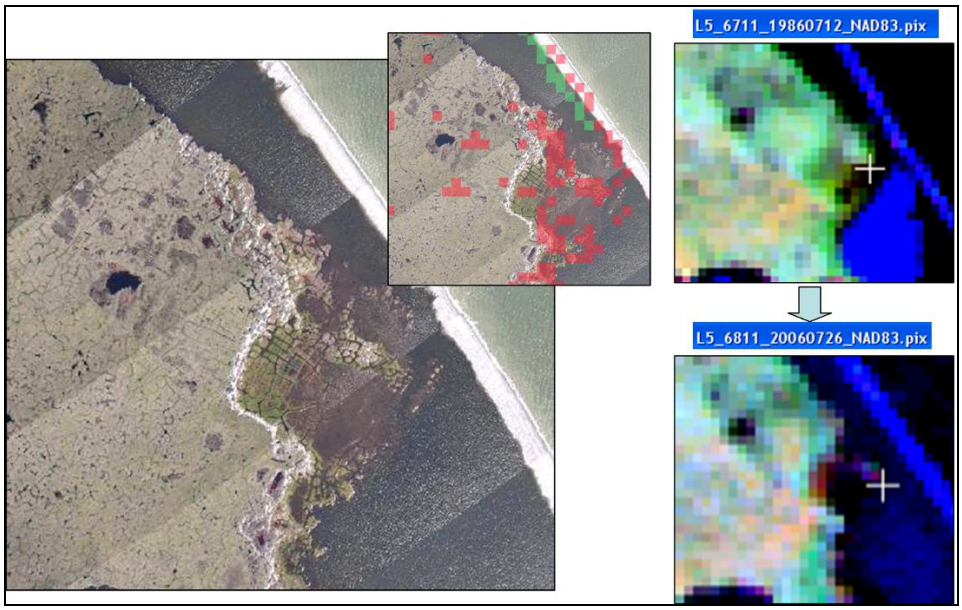

Figure 35 – Negative TC Brightness trend (red) over 2008 air photo shows coastal flooding / erosion. Change is visible in Landsat pair on the right.

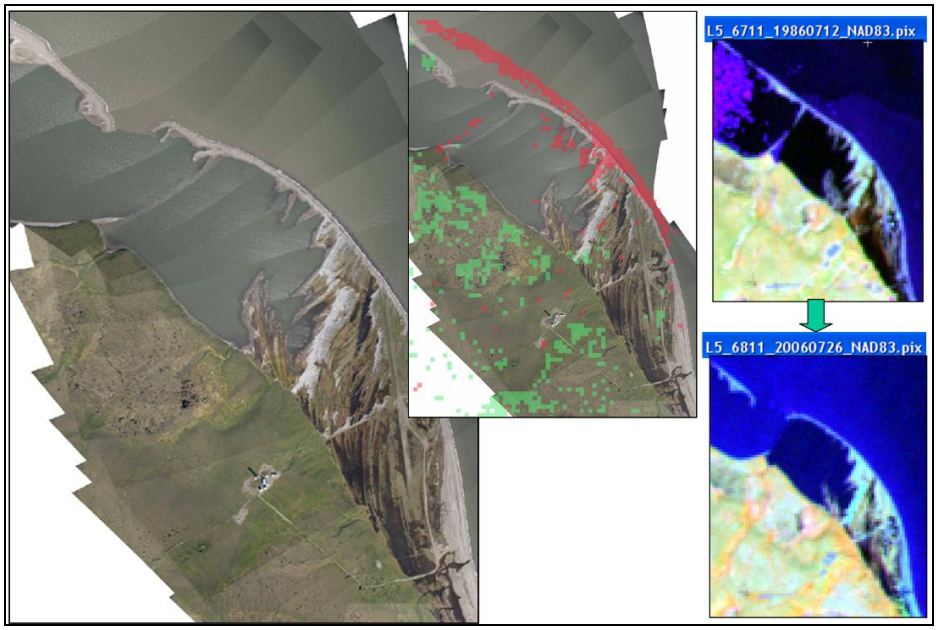

Figure 36 – Negative TC Brightness trend (red) related to coastal erosion. Positive NDVI trend (blue) related to vegetation growth. These changes are evident in the Landsat pair on the right.

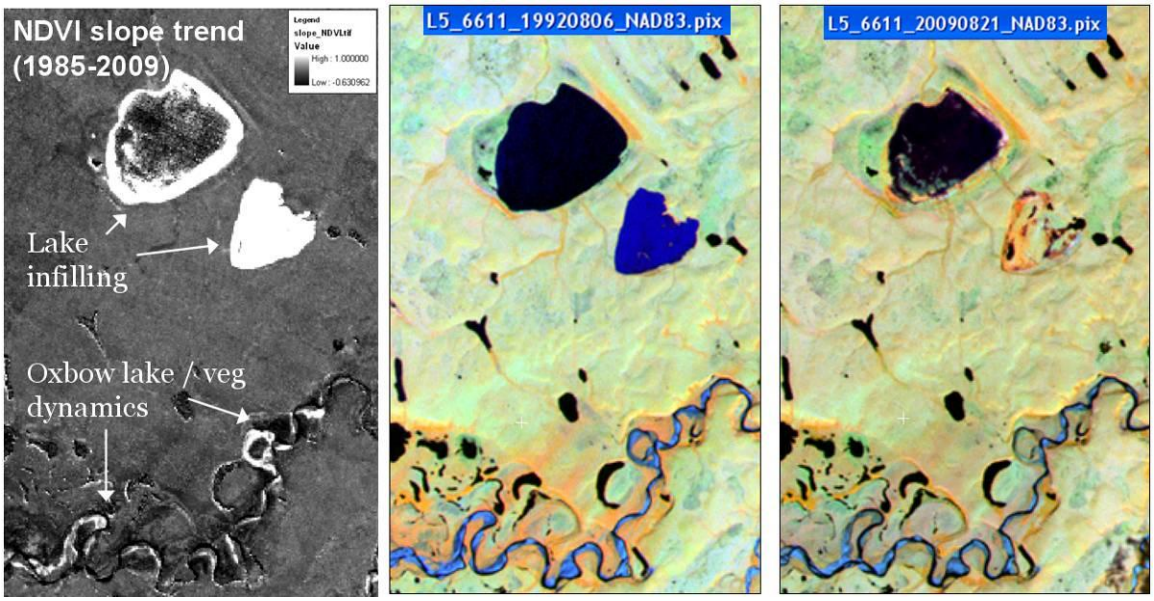

Figure 37 – Lake infilling and oxbow lake dynamics visible in NDVI slope image.

d) Climate Trends for Landsat Observation Period

Some of the trend results, particularly those related to increased growth of vascular vegetation may be attributable to changes in temperature or precipitation that occurred during the 1985-2009 Landsat observation period. Below, we include summaries from various sources of climate data covering Ivvavik. From these, we conclude that:

- Ivvavik suffers spatial and temporal gaps in climate information,
- The area appears to have experienced a warming trend during the winter months
- The trend is weak by comparison to other Arctic regions
- Precipitation, especially during summer, has decreased during 1985-2000

i) North American Regional Reanalysis (NARR) data

The NARR reanalysis product is a continually updated 32 km gridded data set representing the state of the Earth's atmosphere, incorporating observations and numerical weather prediction (NWP) model output dating back to 1948. It is a joint product from the National Centers for Environmental Prediction (NCEP) and the National Center for Atmospheric Research (NCAR).

Since NARR temperature data are missing for the summer months over Ivvavik, only winter trends can be analyzed. Below, two indices are plotted by year: the number of days where temperature falls below 0C, and the cumulative temperature for these days. Both plots suggest a weak warming trend during winters since 1985.

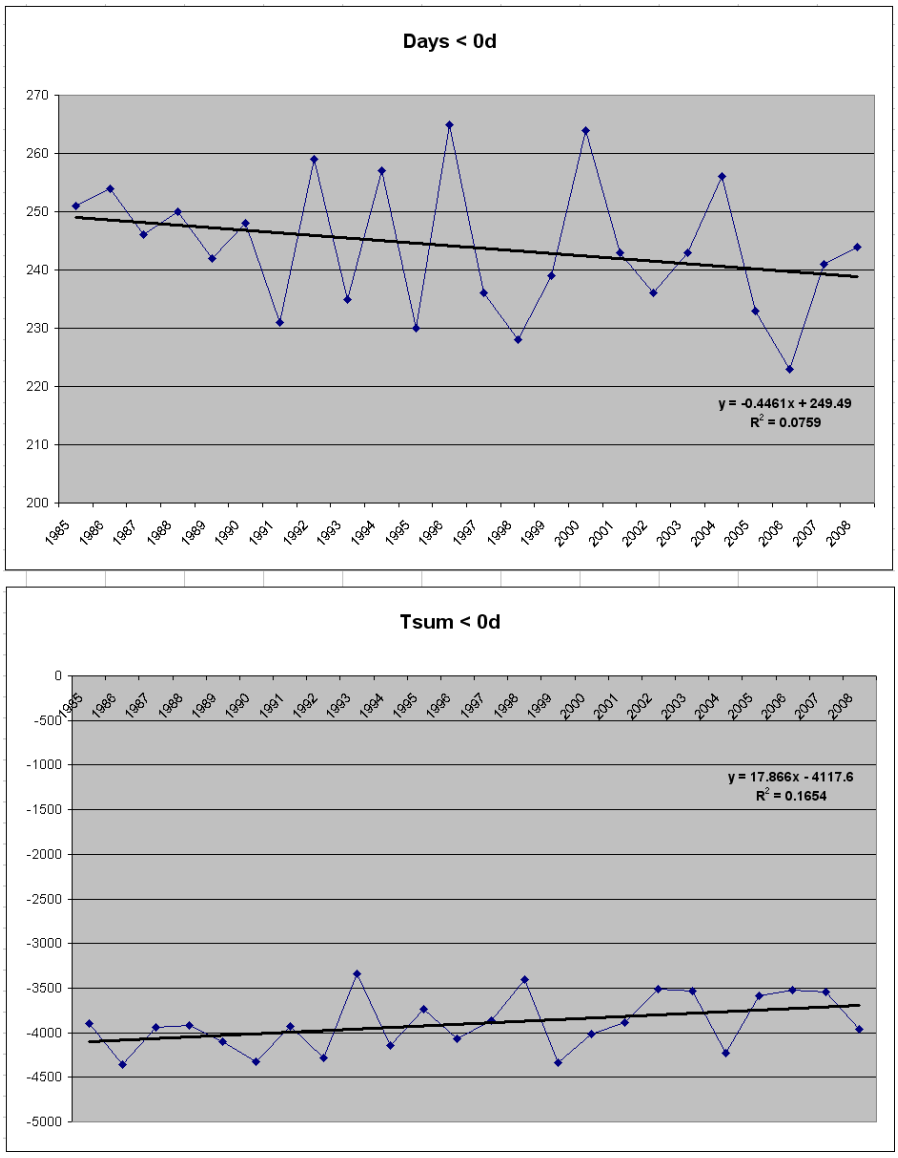

Figure 38 – Winter temperature indices derived using NARR data over Ivvavik.

ii) GISS Surface Temperature Analysis data

The NASA Goddard GISS Surface Temperature (GISTEMP) analysis provides global surface temperature with monthly resolution since 1880, when a reasonably global distribution of meteorological stations was established. The dataset is based on air temperature measurements from the following data sets: the unadjusted data of the Global Historical Climatology Network, United States Historical Climatology Network (USHCN) data, and SCAR (Scientific Committee on Antarctic Research) data from Antarctic stations. The basic analysis method is described by Hansen et al. (1999), with several modifications described by Hansen et al. (2001) also included.

The maps below were prepared using tools at the NASA GISS web site, and show annual summer and winter temperature trends for the period 1985-2009. Note that all three maps, in which station data were smoothed over a 250 km radius, show missing or insufficient data for the area centered over Ivvavik. Areas immediately surrounding Ivvavik show an annual increase in temperature, but that is smaller by comparison to other Arctic regions. Surrounding summer temperatures show a small increase or decrease, while winter temperatures show a marked increase to the east, but a small decrease to the south.

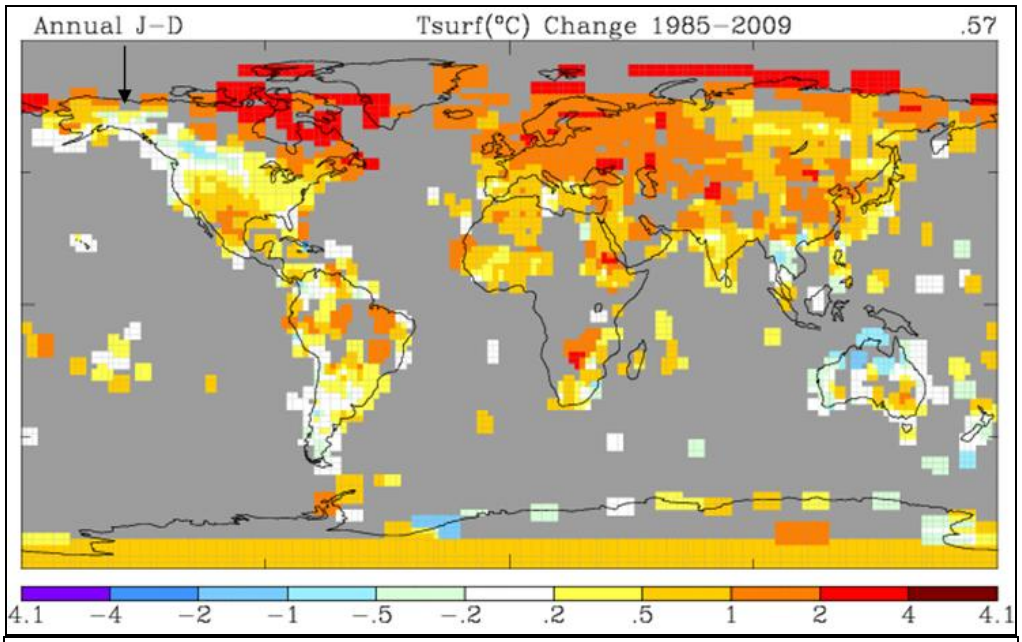

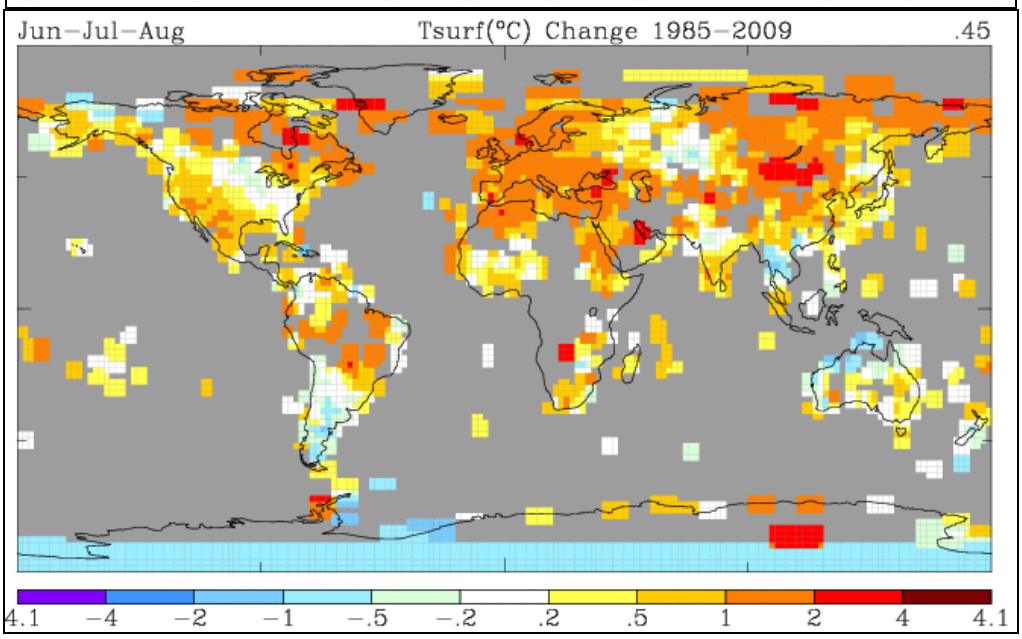

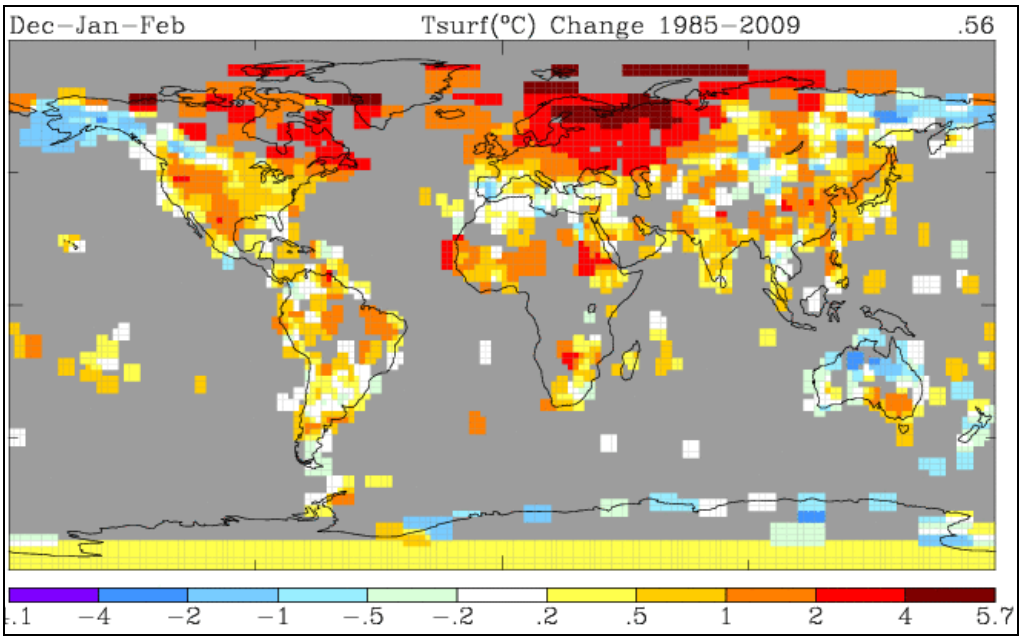

Figure 39 – 1985-2009 temperature changes based on NASA Goddard GISS Surface Temperature (GISTEMP) analysis for the year (top), June-July-August (middle), and Dec-Jan-Feb (bottom).

iii) Temperature from individual climate stations

There are several climate stations within and nearby Ivvavik. Unfortunately, most of these have either short or incomplete records. This problem is reflected in the GISS maps shown above.

A summer warmth index was computed for three stations within or near Ivvavik that have the most complete records (figure 40). From these plots, no long-term trend is observed for the period 1984-2006. Note that Inuvik station, lying 200 km to the east of Ivvavik, shows a strong positive trend in annual temperature (figure 41), which is mostly attributable to warmer winters. This spatial pattern is reflected in the GISS maps above.

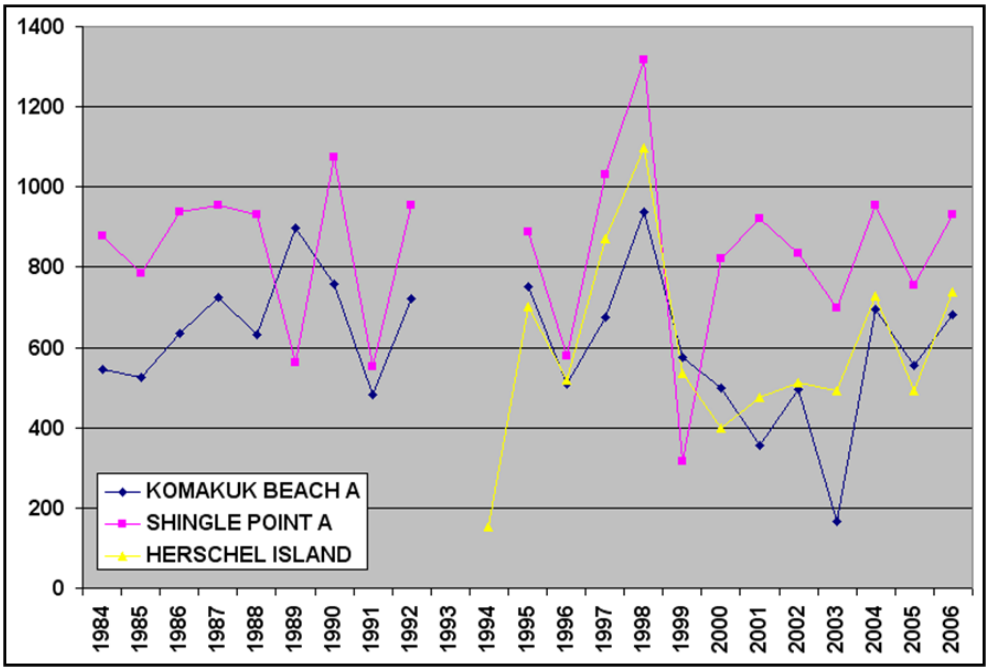

Figure 40 – Summer warmth index computed from Environment Canada weather stations within Ivvavik area (Olthof).

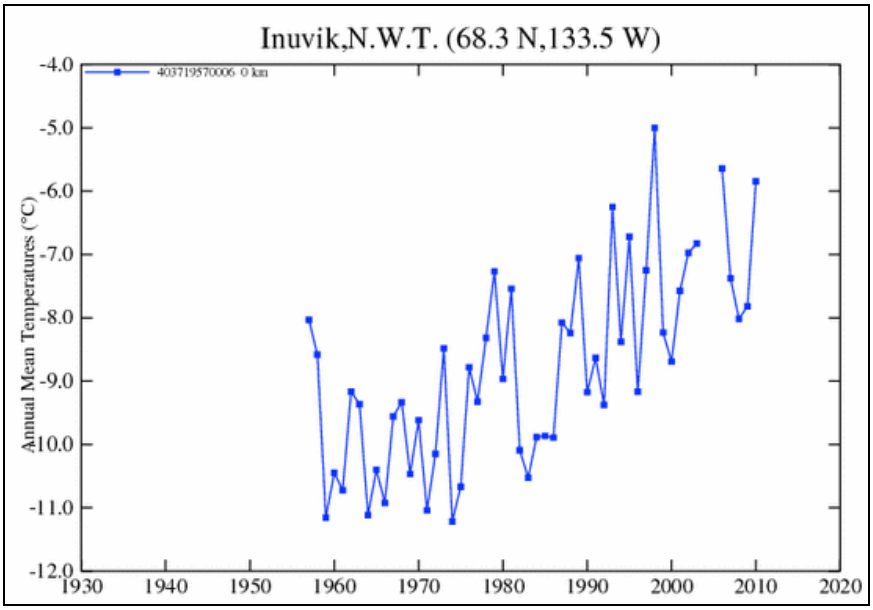

Figure 41 – Mean annual temperature from Inuvik weather station, lying 200 km to the east of Ivvavik.

iv) Rainfall trends

Global, gridded precipitation data have been created for the period 1901-2000 by the Climate Research Unit at the University of East Anglia. The NASA GISS site provides a

tool to generate trends maps from this dataset (http://data.giss.nasa.gov/precip_cru/maps.html). Figure 42 shows the June-August precipitation trend for 1985-2000, and suggests that summer precipitation has decreased in Ivvavik during this period. A weaker decrease (not shown) is also observed for the winter months.

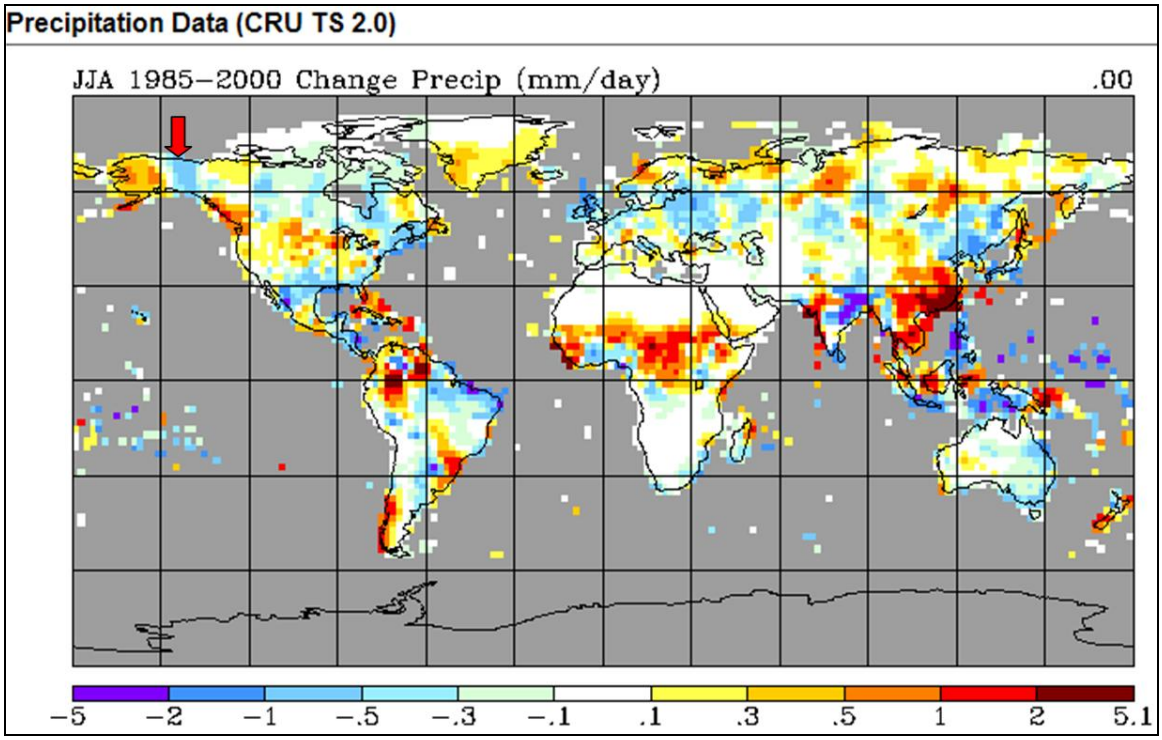

Figure 42: Trend in June-August precipitation for 1985-2000 (CRU dataset ends in 2000).

6. References

Chapin, F. S., III, G. R. Shaver, A. E. Giblin, K. J. Nadelhoffer, and J. A. Laundre. 1995. Responses of arctic tundra to experimental and observed changes in climate. Ecology 76: 694–711.

Fernandes, R., R. Fraser, R. Latifovic, J. Cihlar, J. Beaubien, and Y. Du. 2004. Approaches to fractional land cover and continuous field mapping: A comparative assessment over the BOREAS study region. Remote Sensing of Environment 89: 234−251.

Fraser, R., McLennan, D., Ponomarenko, S., and Olthof, I. 2010. Predictive Ecosystem Mapping over Canadian Arctic National Parks. Submitted to Applied Vegetation Science.

Geoff B. Hill, Greg H. R. Henry. (2010) Responses of High Arctic wet sedge tundra to climate warming since 1980. Global Change Biology.

Goetz, S., A. Bunn, G. Fiske, and R. Houghton. 2005. Satellite-observed photosynthetic trends across North America associated with climate and fire disturbance. Proceedings of the National Academy of Sciences of the United States of America 102: 13521–13525.

Gould, W. A., Mercado Díaz, J. A., and Zimmerman, J.K. 2009. Twenty year record of vegetation change from long-term plots in Alaskan tundra. Presented at the Long Term Ecological Research Network All Scientists Meeting, September 14-16, 2009. Estes Park, CO.

Hill, G.B., and G.H.R. Henry. 2010. Responses of a High Arctic wet sedge tundra to climate warming since 1980. Global Change Biology doi:10.1111/ j.1365-2486.2010.02244.x.

Jia, G.J., H.E. Epstein, and D.A. Walker. 2009. Vegetation greening in the Canadian Arctic related to warming and sea ice decline. Journal of Environmental Monitoring 11: 2231-2238.

Kendall, M.G., and A.S. Stuart. 1967. Advanced theory of statistics, Vol. 2. London: Charles Griffin and Company.

Kennedy, C. 2008. Vegetation Change on Herschel Island and the Ivvavik Coastal Plain. Pg 110-114 in 2007 Yukon North Slope Conference, Keeping Track: Environmental Monitoring and Reporting in Wildlife Management. Summary Report.

Lantuit, H. and Pollard, W.H. 2008. Fifty years of coastal erosion and retrogressive thaw slump activity on Herschel Island, southern Beaufort Sea, Yukon Territory, Canada. Geomorphology, 95(1/2), 84–102.

Myers-Smith, I., Hik, D., Kennedy, C., Cooley, D., Johnstone, J.F., Keney, A.J., and Krebs, C. 2011. Expansion of Canopy-forming willows over the twentieth century on Herschel Island, Yukon Territory, Canada. Ambio 40:610-623.

Olthof, I., and Fraser, R.H., 2007. Mapping northern land cover fractions using Landsat ETM+. Remote Sensing of Environment 107:496-509.

Olthof, I., Latifovic, R., and Pouliot, D. 2009. Development of a circa 2000 land cover map of northern Canada at 30 m resolution from Landsat. Canadian Journal of Remote Sensing 35:152-165.

Selkowitz, D.J. 2010. A comparison of multi-spectral, multi-angular, and multi-temporal remote sensing datasets for fractional shrub canopy mapping in Arctic Alaska. Remote Sensing of Environment 114:1338-1352.

Stow, D.A., B.H. Burns, and A.S. Hope. 1993. Spectral, spatial and temporal characteristics of Arctic tundra reflectance. International Journal of Remote Sensing 14: 2445-2462.

Sturm M., Schimel J., Michaelson G., Welker J. M., Oberbauer S. F., Liston G. E., Fahnestock J., Romanovsky V. E. 2005. Winter biological processes could help convert Arctic tundra to shrubland. BioScience 55, 17–26.

Walker, D.A. 2000. Hierarchical subdivision of Arctic tundra based on vegetation response to climate, parent material and topography. Global Change Biology 6: 19-34.